UNIVERSITY OF GAZİANTEP
GRADUATE SCHOOL OF
NATURAL & APPLIED SCIENCES

AN EXPERIMENTAL INVESTIGATION OF ELECTRICAL DISCHARGE MACHINING (EDM) FAST HOLE DRILLING OF INCONEL 718 & Ti-6Al-4V

M. Sc. THESIS
IN
MECHANICAL ENGINEERING

BY

MUHAMMED ALİ OKKA

JANUARY 2011

An Experimental Investigation of Electrical Discharge Machining (EDM) Fast Hole Drilling of Inconel 718 & Ti-6Al-4V

M.Sc. Thesis

in

Mechanical Engineering

University of Gaziantep

Supervisor

Assist. Prof. Dr Oğuzhan Yılmaz

by

M. Ali OKKA

January 2011

ABSTRACT

AN EXPERIMENTAL INVESTIGATION OF ELECTRICAL DISCHARGE MACHINING (EDM) FAST HOLE DRILLING OF INCONEL718 & Ti6Al4V

OKKA, M. Ali

M.Sc. in Mechanical Eng.

Supervisor: Assist. Prof. Dr. Oğuzhan YILMAZ

JANUARY 2011, 80 pages

Aerospace manufacturing industry demands high level of quality, accuracy, skilled work and precision manufacturing operations. Electrical discharge machining (EDM) which is very prominent amongst the non-conventional machining methods is effectively used in aerospace manufacturing applications. EDM hole drilling is a variation of EDM process and it is preferred to drill holes with high-aspect ratios. This work was undertaken to investigate EDM hole drilling processes and study EDM hole drilling performance on aerospace alloys, namely Inconel 718 and Ti-6Al-4V. Effects of EDM process parameters, such as discharge current, pulse on/off time and capacitance on material removal rates (MRR), electrode wear (EWR) and surface roughness (SR) were analysed throughout the experimental works. The experimental plan was conducted according to the design of experiment (DOE) and the results were statistically evaluated using analysis of variance (ANOVA). Response surface methodology (RSM) was employed in evaluating the drilling performance of the EDM process and mathematical models and optimisation attempts for MRR, EWR and SR were established. The results obtained from the mathematical models and optimisation attempts were verified additional validation experiments.

Key Words: EDM, Hole-drilling, Aerospace Alloys

ÖZET

INCONEL718 & Ti6Al4V ALAŞIMLARINDA ELEKTRİKSEL EROZYONLA İŞLEME YÖNTEMİYLE HIZLI DELİK DELMENİN DENEYSEL İNCELENMESİ

OKKA, M. Ali

Yüksek Lisans Tezi, Makine Müh. Bölümü

Tez Yöneticisi: Yrd. Doç. Dr. Oğuzhan YILMAZ

OCAK 2011, 80 sayfa

Uzay ve Havacılık imalat sanayisi, yüksek kalite, doğruluk, kalifiyeli iş-gücü ve hassas üretim metotlarına rağbet eder. Konvansiyonel olmayan metotlar arasında öne çıkan Elektriksel Erozyonla İşleme (EEİ), uzay ve havacılık imalat uygulamalarında etkin olarak kullanılan metotlardandır. EEİ ile delik delme metodu ise EEİ yönteminin bir varyasyonudur ve boy-çap oranı yüksek olan deliklerin delinmesinde tercih edilmektedir. Bu çalışma, EEİ ile delik delme işlemini araştırmak; uzay ve havacılık uygulamalarında kullanılan Inconel 718 ve Ti-6Al-4V isimli alaşımlarda EEİ ile delik delme performanslarını incelemek üzere gerçekleştirilmiştir. Deneysel çalışmalarla EEİ işleme parametreleri olan deşarj akımı, vurma/dinlenme süreleri ve kapasitansın iş parçası işleme hızının (İİH), elektrot aşınma oranının (EAO) ve yüzey pürüzlülüğünün (YP) üzerindeki etkisi analiz edilmiştir. Deneysel plan deney tasarım metoduna (DTM) göre yürütülmüş ve sonuçlar istatistiksel varyasyon analizi (ANOVA) kullanılarak geliştirilmiştir. Tepki yüzey metodolojisi (TYM), EEİ delme performansının incelenmesi ve matematiksel modellerinin geliştirilmesi ve optimizasyon çalışmalarında, İİH, EAO ve yüzey pürüzlülüğünün optimum değerlerinin bulunması amacıyla uygulanmıştır. Matematiksel modellerden ve optimizasyon çalışmalarından elde edilen sonuçların etkinliği doğrulama deneyleri ile tespit edilmiştir.

Anahtar Kelimeler: EEİ, hızlı delik delme, uzay ve havacılık alaşımları

ACKNOWLEDGEMENTS

Firstly, The author wishes to express his deepest gratitude to his supervisor Assist. Prof. Dr. Oğuzhan YILMAZ for his advice and encouragement during the investigation and fulfilment of this study

The author also would like to special thank to Assist. Prof. Dr. A. Tolga BOZDANA for his invaluable advices and criticism. The author also would like to thank to the all mechanical engineering department lecturers for their advices.Many thanks are to all of the technicians in the departmental work-shop for their cooperation and assisting me in the various laboratory tasks.

I also would like to express my sincere appreciation to all of my friends in University of Gaziantep for colouring my daily live and helped me in one-way or another.

Deepest gratitude is to my parents, who give me a real love, pray, support that all they have. Also a special thanks to my wife for her continuous encouragement and patience.

Finally, I am grateful to TUBİTAK for the financial support during the period of this research work. This work was granted by TUBİTAK 1001 Research Project scheme, No: 108M022.

TABLE of CONTENT

ABSTRACT i
ÖZET ii
ACKNOWLEDGEMENTS iii
TABLE of CONTENT iv
LIST of FIGURE vi
LIST of TABLE viii
NOMENCLATURE x
CHAPTER 1 1
INTRODUCTION 1
1.1 EDM Working Principles 1
1.2 Types of EDM 3
1.3 Application of EDM Hole Drilling 3
1.4 Scope of the thesis 4
1.5 Aim of the Thesis 4
1.6 Outline of the Thesis 5
CHAPTER 2 6
LITERATURE REVIEW 6
2.1 Introduction 6
2.2 General EDM Applications 7
2.3 EDM Fast Hole Drilling 12
2.4 Literature gaps 16
CHAPTER 3 17
EXPERIMENTAL SETUP AND PROCEDURE 17
3.1 Introduction 17
3.2 Design of Experiment 17
3.3 Experimental procedure and set-up 23
3.3.1 Machine and equipments 24
3.3.2 Test pieces 27

3.3.3 Electrodes 29
3.3.4 Experimental Procedure 30
3.4 Experimental Measurements 31
3.4.1 Material Removal Rate (MRR) 31
3.4.2 Electrode Ware Rate (EWR) 31
3.4.3 Surface Roughness (Ra) 32
CHAPTER 4 36
MODELLING AND OPTIMISATION OF THE EDM FAST HOLE DRILLING OPERATIONS 36
4.1 Introduction 36
4.2 Experimental Results of EDM fast hole drilling operations 37
4.3 Mathematical modelling of EDM fast hole drilling process 41
4.3.1 Response Surface Methodology 41
4.3.2 ANOVA Test for the generated mathematical models 47
4.3.3 Predicted and experimental results 51
4.4 Main effects and Interaction plots 54
4.4.1 Effects of EDM input parameters on MRR for D2NiBr 55
4.4.2 Effects of EDM input parameters on EWR for D2NiBr 56
4.4.3 Effects of EDM input parameters on Ra for D2NiBr 57
4.5 Optimization of EDM fast hole drilling process 58
4.5.1 Optimization results of MRR, EWR and Ra for D2NiBr 60
4.5.2 Optimization of MRR, EWR and Ra for D2NiCu 61
4.5.3 Optimization of MRR, EWR and Ra for D2TiBr 62
4.5.4 Optimization of MRR, EWR and Ra for D2TiCu 62
4.6 Validation Experiments 65
CHAPTER 5 67
DISCUSSIONS and CONCLUSIONS 67
REFERENCES 69
APPENDICES 71
Appendix A 72
Appendix B 75
Appendix C 78
LIST OF PUBLICATIONS 79

LIST of FIGURE

Page

Figure 1.1 Proposed model of breakdown phase. (a) Emission of pre-breakdown current and heating at micro peaks. (b) Bubble nucleation at micro-peak. (c) Reaching electron impact criteria at bubble interface. (d) Bubble elongation towards anode. (e) Bubble abridged the inter-electrode gap and fully developed plasma channel at the end of the breakdown phase……. 2

Figure 1.2 a) fuel injector (nozzle), b) turbine blades…… 3

Figure 2.1 Shematic picture of EDM…… 6

Figure 2.2 Working principles of EDM…… 7

Figure 2.3 Different dielectric apply methods (a) flushing dielectric in electrode channel, (b) sucking dielectric, (c) Static, (d) out flushing……... 8

Figure 2.4 (a) Schematic cross-sectional view of EDMed hole (b) Optical view of end of the tool after machining…… 11

Figure 2.5 (a) Micro-EDMed hole at the interface, and (b) micro-EDMed half-hole (c) Two halves of split work-pieces showing micro-holes made by micro-EDM drilling……..……. 11

Figure 2.6 Schematic view of EDM fast hole drilling……..…… 12

Figure 2.7 Schematic diagram of the experimental set-up for EDMBhD process……..…….. 15

Figure 2.8 Assembly of the composite electrode EDM system: (a) system diagram and (b) electrode-motion diagram……... 15

Figure 3.1 Schematic view of experiments……... 24

Figure 3.2 (a) Schematic view of EDM Hole Drilling machine (b) Overall picture of EDM Hole Drilling machine……. 25

Figure 3.3 (a) Overall picture and (b) Control Unit of JS AD-20 EDM……... 26

Figure 3.4 Precious vise and special fixture…….. 26

Figure 3.5 Dimensions of the work pieces and demonstration of the holes in a solid model……..... 29

Figure 3.6 Single-channel (a) brass (b) copper electrodes…… 29
Figure 3.7 SEM images (a) D2NiBr 9-10-11x8 ve (b) D2NiBr 9-10-11x8+10deg……. 33
Figure 3.8 A 3D surface model generated from captured SEM image……. 33
Figure 3.9 Surface roughness (Ra) measurements…… 34
Figure 3.10 Roughness results…….. 34
Figure 3.11 Profile analysis……... 35
Figure 3.12 Linear measurements……. 35
Figure 4.1 Main effects plot of D2NiBr for MRR..... 55
Figure 4.2 Interaction Plot of D2NiBr for MRR..... 56
Figure 4.3 Main effects plot of D2NiBr for EWR..... 57
Figure 4.4 Interaction Plot of D2NiBr for EWR..... 57
Figure 4.5 Main effects plot of D2NiBr for Ra..... 58
Figure 4.6 Interaction Plot of D2NiBr for Ra..... 58
Figure 4.7 Optimization graphs and results of D2NiBr for MRR, EWR and Ra.....……. 61
Figure 4.8 Optimization graphs and results of D2NiCu for MRR, EWR and Ra…… 61
Figure 4.9 Optimization graphs and results of D2TiBr for MRR, EWR and Ra.....……... 62
Figure 4.10 Optimization graphs and results of D2TiCu for MRR, EWR and Ra.....……. 63

LIST of TABLE

Page

Table 3.1 Coded factors of EDM hole drilling machine settings…… 20

Table 3.2 Coded factors value……..……... 20

Table 3.3 Thirty one coded experiments……..……... 21

Table 3.4 Thirty one experiments coded with EDM machine setting. The sequence shown in this table also was used in the conducted experiments…… 22

Table 3.5 Thirty one experiments with their exact values…….. 23

Table 3.6 Chemical composition of Inconel 718 (wt. %) …….. 28

Table 3.7 Chemical composition of Ti6Al4V (wt. %) ……... 28

Table 3.8 Properties of Inconel 718……..…….. 28

Table 3.9 Properties of Ti6Al4V……..……... 28

Table 3.10 Major properties of electrode materials…… 29

Table 3.11 Experimental variables and constants…..……. 31

Table 4.1 Experimental results of MRR, EWR and Ra for D2NiBr..... 37

Table 4.2 Experimental Results of MRR, EWR and Ra for 2mm D2NiCu..... 38

Table 4.3 Experimental Results of MRR, EWR and Ra for D2TiBr..... 39

Table 4.4 Experimental Results of MRR, EWR and Ra for D2TiCu..... 40

Table 4.5 Linear and exponential functions..... 42

Table 4.6 Response equations for D2NiBr……..……... 42

Table 4.7 Mathematical Models of In718-Brass MRR……... 43

Table 4.8 Mathematical Models of IN718-Copper MRR……... 43

Table 4.9 Mathematical Models of Ti64-Brass MRR……. 43

Table 4.10 Mathematical Models of Ti64-Copper MRR…… 44

Table 4.11 Mathematical Models of IN718-Brass EWR…… 44

Table 4.12 Mathematical Models of IN718-Copper EWR……. 44

Table 4.13 Mathematical Models of Ti64-Brass EWR……... 45

Table 4.14 Mathematical Models of Ti64-Copper EWR..... 45

Table 4.15 Mathematical Models of IN718-Brass Ra…… 45

Table 4.16 Mathematical Models of IN718-Copper Ra……. 46

Table 4.17 Mathematical Models of Ti64-Brass Ra……..... 46
Table 4.18 Mathematical Models of Ti64-Copper Ra…… 46
Table 4.19 D2NiBr MRR ANOVA test……..…… 48
Table 4.20 D2NiBr EWR ANOVA test……..…… 48
Table 4.21 D2NiBr Ra ANOVA test……..…… 49
Table 4.22 Reduced response equations for D2NiBr…….. 50
Table 4.23 Experimental and predicted results; percentage errors of D2NiBr... 51
Table 4.24 Experimental and predicted results; percentage errors of D2NiCu.. 52
Table 4.25 Experimental and predicted results; percentage errors of D2TiBr... 53
Table 4.26 Experimental and predicted results; percentage errors of D2TiCu... 54
Table 4.27 Optimization experiments results of EDM hole drilling..... 64
Table 4.28 Validation experiments input values..... 65
Table 4.29 Comparisons of the validation results..... 65

NOMENCLATURE

EDM…….……..	Electrical Discharge Machining
IN718……..	Inconel 718
Ti64.....….....	Ti-6Al-4V
NiBr…….	IN718 EDM with Brass electrode
NiCu……	IN718 EDM with Copper electrode
TiBr…….....	Ti64 EDM with Brass electrode
TiCu…….....	Ti64 EDM with Copper electrode
DOE…….…….....	Design of Experiments
RSM…….…….....	Response Surface Methodology
MRR…….....	Material Removal Rate
EWR…….....	Electrode Ware Rate
Ra…….....	Surface Roughness
SEM…….....	Scanning Electron Microscopy
ANOVA……..	Analysis of Variance

CHAPTER 1

INTRODUCTION

Aircraft jet and gas turbine engines are working in harsh environments and they must sustain high reliability. Therefore, engine components are made from super alloys, which have special mechanical and chemical properties, such as, high strength, high hardness, high melting point, low thermal conductivity and corrosion resistivity etc. Inconel 718 and Ti-6Al-4V are commonly used super alloys for aeroengine components. These alloys are known as hard-to-machine materials. The traditional production methods are in general not sufficient to machine these materials. Instead, non-traditional methods like EDM, Electrical Chemical Machining (ECM), abrasive water-jet machining and laser machining have been developed to machine these materials. EDM is one of the most popular methods among non-traditional production methods.

EDM has an ability to machine any electrical conductive materials regardless of their mechanical and chemical properties. Therefore, using EDM method, it is possible to machine high strength and very hard materials as well as materials with high melting points.

1.1 EDM Working Principles

EDM is among the earliest non-traditional manufacturing process, having an inception 50 years ago in a simple die-sinking application. EDM is a thermal material removal process by melting and, partially, vaporization of the work-piece material. Source of the energy used for melting and vaporization is found in the form of heat, generated by electrical discharges and sparks between two electrodes in close proximity. The electrodes (tool electrode and work-piece) are immersed in dielectric liquid or flowing pressurized dielectric medium. Electrical discharge occurs when the dielectric is broken down by the application of voltage pulse. Some of the released energy during discharge is transferred to the electrodes and results in the heating of

highly localized regions of the electrodes. When the temperature of the heating region exceeds melting temperature of the electrodes, material removal starts in size of very small particles. Molten and/or vaporized particles (debris material) are washed away from the sparking area by the continuously flushing dielectric fluid. Flowing pressure of the dielectric fluid should be used in an appropriate value, high pressurized fluid result in vanishing the influence of electrical sparks, and removed together with debris particles, however, low pressure flow result in rising debris concentration in sparking area and cause secondary discharge, arc, and short circuit. In EDM process, mechanical properties of the work-piece do not affect the machining process. Thermal properties such as melting point, boiling point, and electrical conductivity of work-piece materials affect the machining characteristics. The material removal rate of EDM process is primarily determined by the electrical conductivity and melting temperature of the work-piece material. A work-piece with higher electrical conductivity and lower melting temperature can be machined more efficiently [1]. Schematic view of EDM working principle shown in Figure 1.1

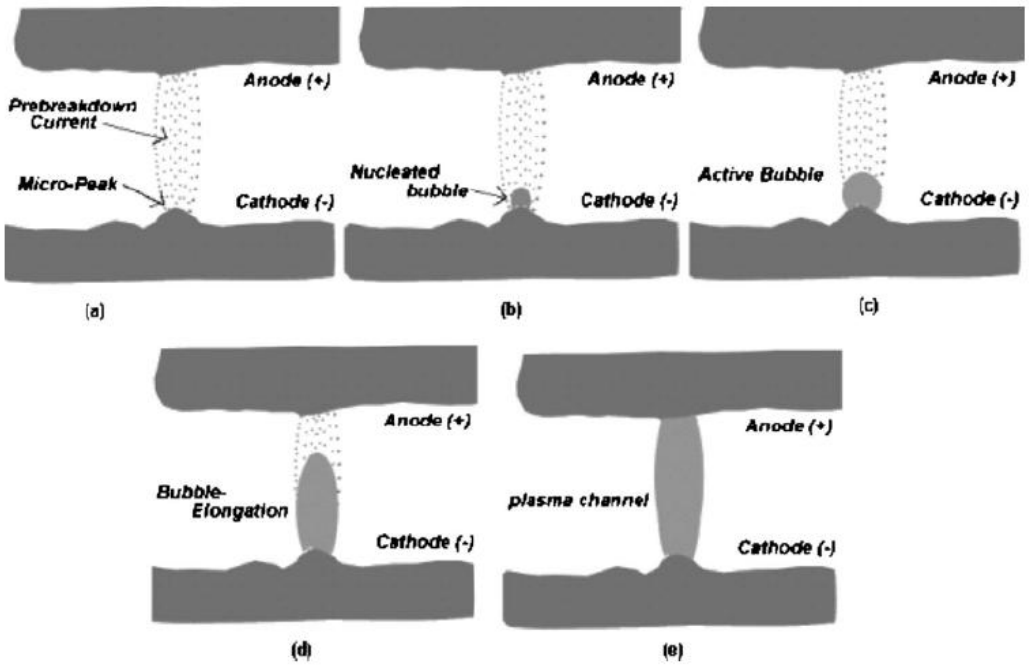

Figure 1.1 Proposed model of breakdown phase. (a) Emission of pre-breakdown current and heating at micro peaks. (b) Bubble nucleation at micro-peak. (c) Reaching electron impact criteria at bubble interface. (d) Bubble elongation towards anode. (e) Bubble abridged the inter-electrode gap and fully developed plasma channel at the end of the breakdown phase. [1]

1.2 Types of EDM

There are three main types of EDM;

- Die sink EDM.
- Wire EDM.
- EDM hole drilling.
- EDM Milling

Die sink EDM is used for mould cavities. Wire EDM is used for cutting plates. This process is used to cut plates as thick as 300mm and to make punches, tools and dies from hard metals that are too difficult to machine with other methods. The wire, which is constantly fed from a spool, is held between upper and lower diamond guides. EDM hole drilling has mainly same principle with other two methods. The main differences of the EDM hole drilling from the others are;

- Use of high pressure (70-100 Bar) dielectric pump.
- Using cylindrical, hollow, rotating electrode.
- High electrode feed rate (controlled by a fast response servo)

These properties provides fast hole drilling ability to EDM about 1mm/sec. hole sizes vary from 0.4mm to 3mm diameters with 150/1 depth to height ratio.

1.3 Application of EDM Hole Drilling

There are many products produced with EDM hole drilling process. Some of them are: fuel injectors, cutting tools, medical equipment, optical apertures, micro pipettes and aerospace components. It is one of the few manufacturing processes that can be applied to the drilling of precision small holes in a number of parts, including turbine blades shown in Figure 1.2

Figure 1.2 Fuel injector (nozzle) and turbine blades

Turbine blades are the most critical components of aeroengine and have crucial role in producing engine thrust. These components are subject to high temperature, high pressure while the engine is working. Therefore, they need to be cooled down in order to decrease the effect of temperature. To do so, thousands of cooling holes are drilled on these components in order to reduce the heat. The most practical method to produce these holes is EDM method. Drilling of these cooling holes takes great amount of production time for turbine blades. Researchers try to reduce this time with producing high quality and low cost of production. Thus, output parameters (MRR, EWR and Ra) have been tried to be optimized.

1.4 Scope of the thesis

Drilling of high-aspect ratio holes with high speed is always a challenge due its difficult manufacturability and cost factors. EDM hole drilling has been extensively used to perform this task within desirable levels. New trends in using special materials and tough geometrical constraints, such as very small diameter holes (less than 1 mm) and deep holes make this task more complicated. Such holes have been seen on different parts and components which are used for different purposes. For instance, small holes on diesel engine ejectors, ventilating holes on metal dies, holes on medical components and turbine blade cooling holes are the most favourable examples. Drilling of these holes with high dimensional precision, at higher efficiency and with cost-effective way is a state-of-the-art. This research work focused on investigating EDM drilling of holes with macro and micro levels on difficult-to-cut materials. The investigation covered extensive experimental work. Optimization and mathematical modelling of EDM hole drilling process was also covered in order to obtain precise hole drilling process with high.

1.5 Aim of the Thesis

The primary aim of this study is to increase the efficiency of EDM drilling on aerospace alloys. Aerospace manufacturing industry always needs more precise and efficient manufacturing methods as well as time-cost effective. This work primarily targets aerospace manufacturing industry and promises better, reliable and efficient EDM drilling processes for micro and macro scale holes.

1.6 Outline of the Thesis

This thesis starts with the introduction chapter that includes what the presented work is about, the scope and the aims to be achieved. The related literature is reviewed and discussed in next chapter. The third chapter covers the experimental setup and the procedure followed. Chapter three also gives detail about the design of the experiments, how these experiments were conducted and which tools/equipments were used in the experiments. Chapter four presents the modelling of EDM hole drilling processes, experimental and predict results and discussions about them. Chapter five includes the conclusions and the future work.

CHAPTER 2

LITERATURE REVIEW

2.1 Introduction

EDM based on the erosion of metals by spark discharge. It is known that when two current-conducting wires are allowed to touch each other, an arc is produced. If we look closely at the point of contact between two wires, it is noted that small portion of the metal has been eroded away, leaving a small crater. The basic EDM system consist of a shaped tool (electrode) and work-piece which is connected to a DC power supply and placed in a dielectric media in a fluid form. When the potential difference between the tool and the work-piece is sufficiently high, a transient spark discharges through the fluid, removing a very small amount of metal from the work-piece surface. In general, EDM machines can supply capacitance discharge which is repeated at rates of between 50kHz and 500kHz, with voltages usually ranging between 50-380 V and currents from 0.1A to 500 A. The work-piece is located within a tank containing the dielectric fluid, and its movement controlled by numerically control systems. The gap between the tool and the work-piece (overcut) is critical; thus the downward feed of the tool is controlled by a servomechanism, which automatically maintains a constant gap. A schematic representation of a die-sinking EDM and its units are shown in Figure 2.1. Figure 2.2 depicts working principles of a typical EDM operation.

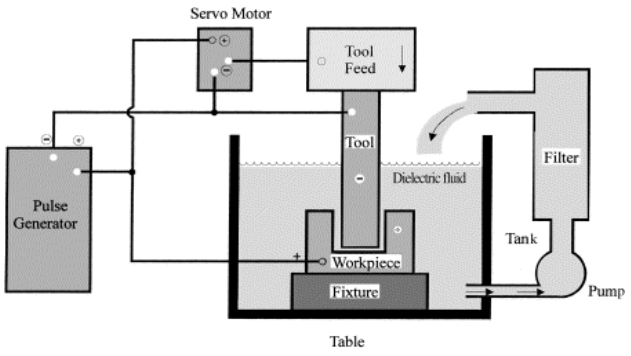

Figure 2.1 Shematic picture of EDM

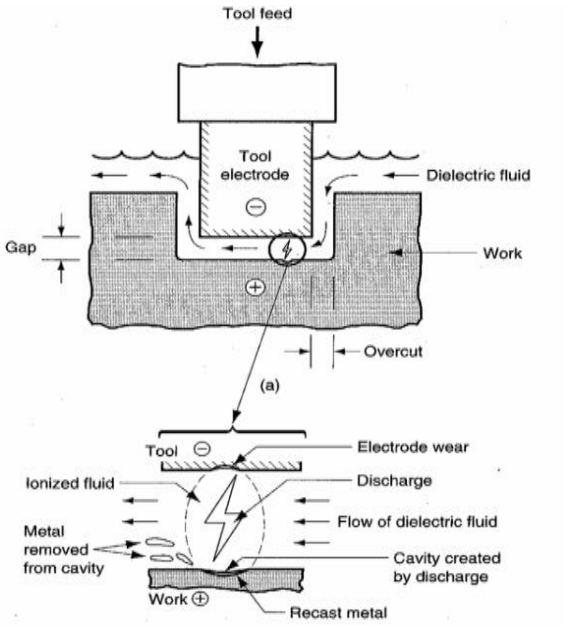

Figure 2.2 Working principles of EDM

In EDM process, any type of conducting materials can be used as the workpiece materials regardless of its hardness. Melting point and thermal conductivity are the two curucial physical properties that determine the volume of metal removed per discharge. Since the process does not involve mechanical energy, hardness, strength and toughness are avoided during the process. The discharge is usually controlled by voltage and current that have effects on the material removal rate. [3]

In the following sections, the related literature are discussed and the contributions of the researches on EDM and EDM hole drilling are summarized. Although there are considerable amount of works on EDM and its applications, EDM hole drilling has been focused on a specific area of the EDM process. Therefore, only few substantial works about EDM are stated in this chapter and the rest covers the works related to EDM hole drilling. Finally, the gaps which have been found in the related literature are revealed. The aim of this research work is to cover these gaps which determined the border of this study.

2.2 General EDM Applications

EDM has been extensively used in die/mold industry. Recent technological achievements and needs have directed this non-conventional process to be adopted in widespread industries, medical, aerospace, tool-making etc. Most of the EDM works

in the literature have involved controlling of process parameters and aimed to obtain best conditions. During the process, the most important factor is controlling the amount and time of discharge since the erosion can only take place from both material and electrode by released energy from this discharge. For instance, Ergün and Çoğun [4] investigated main EDM machining performance outputs, namely work piece removal rate, electrode wear rate, relative wear, crater geometry, work piece surface roughness, micro hardness and microstructure characteristics. Different dielectric methods (flushing, suction and static) as Figure 2.3 and varying machining parameters, such as Current (I, A) and pulse-on (Ton, μs), pulse-off (Toff, μs).

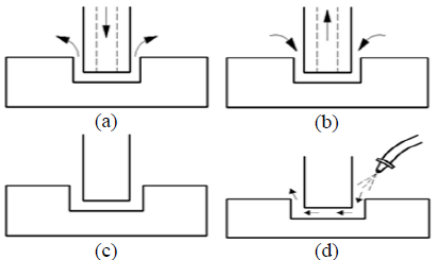

Figure 2.3 Different dielectric apply methods (a) flushing dielectric in electrode channel, (b) sucking dielectric, (c) Static, (d) out flushing [4]

MRR and EWR are the most important criteria which directly influence the performance of an EDM process. Therefore, considerable amount of research have been focused on which operational factors are affecting these outputs using different industrial materials. Khan [5] worked on parameters which are cause of different EWR and MRR during EDM of aluminium and mild steel using copper and brass electrodes. This research work compared copper and brass electrodes. According to the work, EWR increases with increase in current and voltage. The wear ratio (WR) increases with increase in current and gap voltage (Vg). The MRR increases sharply with increase in current. The highest MRR was obtained using a brass electrode during the machining of aluminium.

One of the application industries of EDM is aerospace and EDM has a vital role in this sector while machining of difficult-to-cut materials (Titanium and Nickel alloys). These materials are the two key materials due to their extensive properties. These alloys have high corrosion resistivity, high hardness, high melting point and low weight. Hasçalık and Çaydaş [6] investigated the EDM of Ti-6Al-4V (Ti64) with

different electrode materials namely, graphite, electrolytic copper and aluminium. Process parameters such as, I (A) and Ton (μs) were performed to explore the influence of EDM parameters on various aspects of the surface integrity of Ti64. Scanning electron microscopy (SEM), X-ray diffraction (XRD), energy dispersive spectrograph (EDS) and hardness analysis were performed. The MRR, EW and Ra are increasing with process parameters for each electrode material except the prolonged pulse duration. Graphite electrode gives the highest MRR, followed by electrolytic copper and aluminium. Graphite exhibits the lowest EWR due to higher melting point at all the applied condition. Aluminium electrode exhibits the best performance with regard to surface finish.

EDM related works involves experimental analysis and the experiments in these studies must be very well-planned and conducted in order to investigate necessary parameters. To do that, some statistical techniques have developed and they have been used for modelling of experiments. The minimum number of experiments, the order of the experiments and controlled parameters can be determined using these software(s). Another important facility of these approaches is the mathematically modelling of the process and derives a mathematical formula including operational parameters in the process. Tomadi [7] developed a mathematical model to find the effects of EDM working parameters on MRR, EWR and surface roughness (Ra) with DOE (full factorial method) and ANOVA. EDM working parameters were I(A), Ton(μs), Toff(μs), V(Volt) and duty factor. WC is used as work piece. Ra was found to be mostly effected by voltage then Ton, MRR was mostly affected by Ton, Voltage, Current. EWR was influenced by Toff.

Habib [8] has highlighted the development of a comprehensive mathematical model for correlating the interactive and higher order influences of various EDM parameters through response surface methodology (RSM). The analysis of variance (ANOVA) was used. Optimal combination of these parameters was obtained for achieving controlled EDM of the work pieces. The analysis of the experimental observations demonstrated that the MRR, EWR, gap size and Ra in EDM. The results showed that the MRR increased with an increase of Ton (μs), Toff (μs) and relatively with Vg (V). EWR increased with an increase of both Ton (μs) and I (A) and decreases Vg (V). The gap size increased with the increase of Ton (μs), I (A) and

Vg (V). Finally, the Ra increased with the increase of Ton (μs), I(A) and Vg (V). Investigations were carried out for analysis of the control conditions needed for the control of the MRR, EWR, gap size and Ra

Deniz and Çoğun [9] generated mathematical models with RSM to find the effect of EDM working parameters on working performance parameters and making regression analysis and optimization with using MINITAB software. Ra, MRR and EWR were the dependent variables and I(A), Ton(μs), Toff(μs), working depth(h) were working parameters. In this study, acceptability of mathematical modeling was controlled by F-test and ANOVA. Mathematical models of MRR, EWR and Ra were obtained. Also optimization of maximum MRR, minimum TWR and minimum Ra was made.

Tsai and Wang [10] have developed a Semi-empirical model of surface finish on electrical discharge machining. The parameters of the model, such as peak current, pulse duration, electric polarity, and properties of materials, have been initially screened by the design of experiment procedure. Then, they have been systematically analyzed and later verified by making use of the Taguchi method. In this study, two levels of experimental work were needed to establish the semi-empirical model. Three types of materials, namely copper, graphite, and silver–tungsten alloy, were used for the tool; while three different grades of steel were used for the work piece and generate Semi-empirical model after experiments.

Pradhan [11] mentioned about the influence of micro-EDM working parameter; I(A), Ton(μs), Toff(μs), Flushing Pressure (Pr) and Duty-factor (t), on working performance; MRR, TWR, Over Cut(OC), (figure 2.4). In this study, Ti64 was used as work piece and brass was used as electrode. DOE was used with ANOVA and S/N ratio graph. The significant process parameters and the optimal combination level of machining parameters were obtained. Mathematical models have been developed to establish the relationship between various significant process parameters and micro-EDM performance criteria. In this study, also white layer and surface topography were produced to examine. From the experiments, Ton (μs) was the most effective micro hole EDM drilling parameter for Ti64. TWR was mostly influenced by I(A).

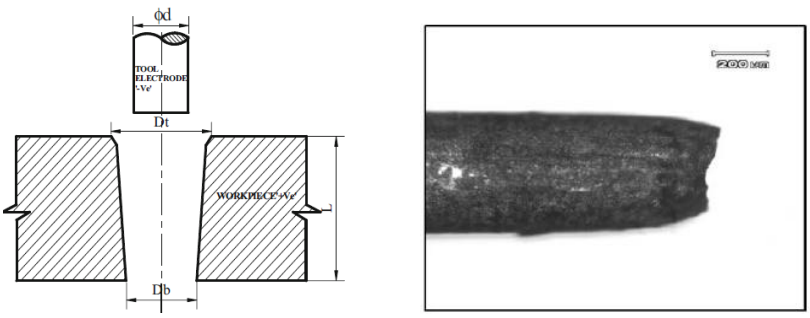

a b

Figure 2.4 (a) Schematic cross-sectional view of EDMed hole (b) Optical view of end of the tool after machining [11]

Puranik [2] has analyzed of accuracy of high-aspect-ratio holes generated using micro-electric discharge machining drilling as figure 2.5. This study showed that the length to diameter ratio of over 25/1 while controlling the regular process parameters. Puranik used the DOE method with five input parameters that influence the accuracy and aspect ratio of the micro-EDMed holes as: (1) electrode rotation; (2) feed velocity; (3) Vg(V); (4) capacitance(μF); (5) resistance. Puranik also used ANOVA with 77% R^2 safeness. The mechanism of surface generation was significantly influenced by debris accumulation and its disposal in the micro-EDM process. The statistical analysis of the results showed that Vg(V) was one of the most significant factors influencing the accuracy of holes in micro-EDM drilling up to a depth of 5.0mm.

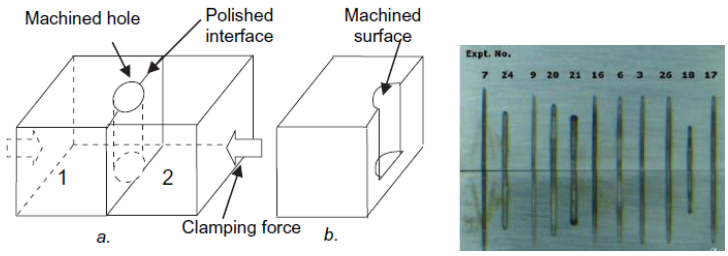

c.

Figure 2.5 (a) Micro-EDMed hole at the interface, and (b) micro-EDMed half-hole (c) Two halves of split work-pieces showing micro-holes made by micro-EDM drilling [2]

Yan [12] described the characteristics of the hole of work-piece carbide by EDM with a copper tool electrode. This study aimed to obtain minimal expansion of the machined micro-hole and minimal tool electrode wear rate to secure a high precision

micro-hole in the carbide. From the experimental results, some important consequences were summarized as follows: When machining micro-holes in carbide with copper tool electrode, positive-polarity machining must be used: this differs from the negative-polarity machining used commonly in normal EDM. Increasing the rotational speed of the tool electrode can improve the debris discharge and reduce the expansion of the micro-hole, but it has no great effect on the tool electrode wear rate.

2.3 EDM Fast Hole Drilling

EDM fast hole drilling is a different variation of EDM processes, i.e. die sink EDM and wire EDM. Although EDM fast hole drilling shown in Figure 2.6 uses the same principles as other EDM methods, a constantly rotated hollow electrode and pumping of dielectric fluid through the electrode tube are the two distinct features. The rotating electrode helps in producing concentricity, causing even wear, and helps in the flushing process. The high flushing pressure through the centre of the electrode tends to stiffen it. Also, the dielectric being forced out of the hole produces a centring effect upon the electrode. With the aid of the electrode guide and the flushing effects on the electrode, EDM drilling can penetrate much deeper in higher rates than almost any other drilling method. Drilling rates up to 1mm/second can be achieved and the hole size is generally between 0.15 to 3 mm, with a length to diameter ratio of over 150:1. This process has been alternatively used for producing holes in turbine blades, fuel injectors, medical equipments, cutting tool coolant holes, hardened punch ejectors, plastic mold vent holes and wire EDM starter holes. [13]

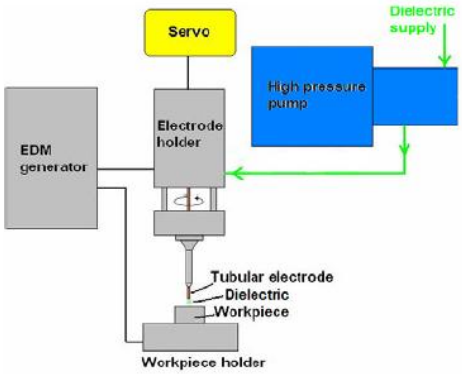

Figure 2.6 Schematic view of EDM fast hole drilling. [13]

Bigot [14] studied on a method for machining parameters optimization in EDM drilling with 0.170mm diameter electrodes. DOE method was used to reduce the number of experiments. Bigot measured EWR by assessing the difference in length of the electrode before and after machining. The control factors of the experiments were electrode polarity (negative or positive), peak current, ignition voltage, pulse-on time, pulse-off time, capacitance and gap. Outputs of this research were MRR, EWR and Ra. Optimum results were obtained if the electrode was connected to negative polarity.

Soni [15] has discussed electrode rotation effects on titanium with rotary EDM. Stationary electrode, rotational electrode and orbital rotated electrode were compared as Figure 2.7. Out of roundness, over cut, blind hole and true hole were the outputs. The minimum over cut was obtained at stationary electrode. The maximum out of roundness was obtained with stationary electrode, when the rotation of electrode (rpm) was increased than over cut and out of roundness increased. If the Ton (μs) increased than over cut decreased. Also Soni made explanation about craters which were generating on EDM machined surface. Craters formed because of melted metal, also low Ton (μs) produced small craters and good surface quality.

Kuppan [16] studied on influence of EDM process parameters in small deep hole drilling of Inconel 718. The parameters such as peak current, pulse on-time, duty factor and electrode speed were chosen to study the machining characteristics. An electrolytic copper tube of 3 mm diameter was selected as a tool electrode. The experiments were planned using central composite design (CCD) procedure. The output responses measured were material removal rate (MRR) and depth averaged surface roughness (DASR). Mathematical models were derived for the above responses using response surface methodology (RSM). The results revealed that MRR is more influenced by peak current, duty factor and electrode rotation, whereas DASR is strongly influenced by peak current and pulse on time. Finally, the parameters were optimized for maximum MRR with the desired surface roughness value using desirability function approach. The following conclusions can be derived based on the results and discussion for the Inconel 718 material with copper electrode in the investigated range: The MRR increases with the increase in peak current, duty factor and electrode speed. Whereas the individual, higher-order and

interaction effects of factors peak current and pulse on-time, and interaction effect between peak current and electrode rotation have significant contribution on surface roughness model.

Wang and Yan [17] have optimized the blind-hole drilling of Al2O3/6061Al composite using rotary electro-discharging machining (Figure 2.7) by using Taguchi methodology. There are seven different input parameter used; polarity, I (A), Ton (μs) and Vg (V), rotational speed (rpm) of the electrode, Pr (kPa), and the channel number of the electrodes. Experimental results confirmed that the revised copper electrode with an eccentric through-hole had the optimum performance for machining from various aspects. Three observed values, MRR, EWR, and SR verified this optimization of the machining technique. In this study, semi-empirical equations derived that contain all of the machining characteristics. R^2 which was generated with semi-empirical formula was changing with %79 to 90%.

Leao and Pashby [18] made optimization of EDM fast hole drilling through evaluation of dielectric and electrode materials. This optimization made with RSM, a series of studies have been carried out with the purpose of optimizing the drilling process through the evaluation of water-based dielectric and an electrode material different from the standard materials of dionised water-brass, through analysis of machining time, EW, Ra and dimensional accuracy. Experiments designated, good drilling rates and achieve reduction in electrode wear of nearly %50.

Kumagai [19] made operation parameter optimization for fabrication of a narrow, deep hole in metal by electrical discharge machining using a dielectric-encased wire electrode in a dielectric pipe, which serves as a jacket as Figure 2.8. In this study, the optimum width of the current pulse applied, the optimum distance between the tips of the electrode and the jacket, and the optimum vibration amplitude of the electrode feed control was determined. This optimization provides ~35% higher machining speed and ~40% less electrode wear than the parameters used in the previous study.

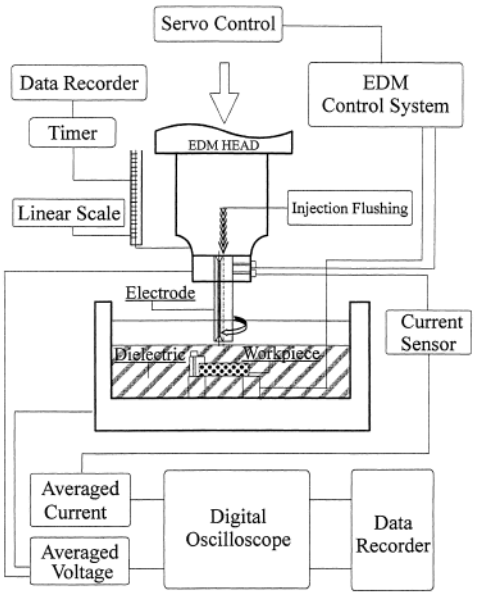

Figure 2.7 Schematic diagram of the experimental set-up for EDMBhD process. [17]

Jahan and Rahman [20] have studied on the quality micro-hole machining of tungsten carbide by EDM hole drilling process using transistor and RC-type pulse generator. This study investigates the influence of major operating parameters on the performance of EDM hole drilling of WC with focus in obtaining quality micro-holes in both transistor and RC-type generators. Experimental investigations were conducted with view of obtaining high-quality micro-holes in WC with small spark gap, better dimensional accuracy, good surface finish and circularity.

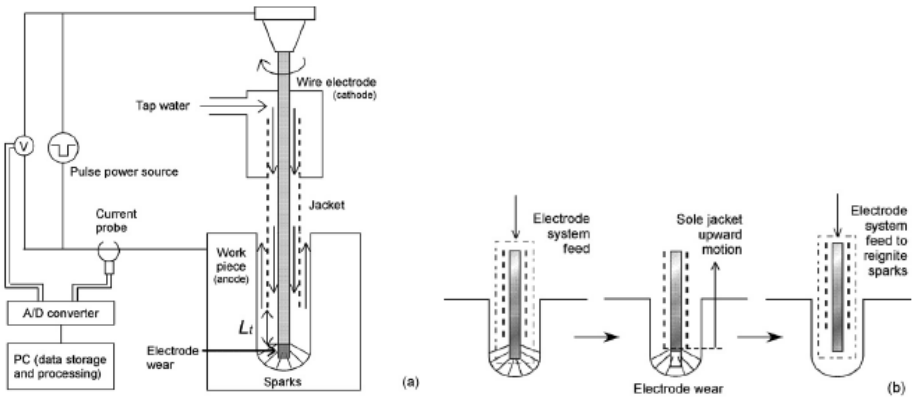

Figure 2.8 Assembly of the composite electrode EDM system: (a) system diagram and (b) electrode-motion diagram. [19]

2.4 Literature gaps

The related literature have been summarized and discussed in this chapter. Although the literature works have minor or major contributions to the technological developments of EDM and EDM hole drilling, there are still missing gaps which must be filled. It can be clearly seen that the works focused on a specific material, electrode, and electrode diameter and process conditions. The works either investigated process parameters or optimizing them. Works on Ti6Al4V are limited and yet Inconel 718 material has not been studied very well. These alloys are crucial in aerospace and medical sectors and EDM is the key manufacturing process in order to produce difficult shapes and micro-macro scale holes. There is still need to have such a work that reveals EDM hole drilling performance in various diameters from micro to macro scale. Electrode type has a significant impact on proper EDM conditions but however, comparative investigations of electrode materials in EDM hole drilling still remains obscure. Mathematical modelling of micro-macro scale EDM hole drilling and optimization of these processes would be valuable contributions. Such a contribution will be a positive impact on the manufacturing capability of drilling thousands of small holes on a part, i.e Turbine blade, combustor etc.

CHAPTER 3

EXPERIMENTAL SETUP AND PROCEDURE

3.1 Introduction

This chapter includes the details of techniques, methods and equipment, which were used in the conducted experiments. Statistical techniques have been preferred in order to model the experiments and extract the relationship of the experimental variables as well as optimization. Design of experiment (DOE) method was used to determine the number and the random sequence of experiments in which the best possible results can be obtained. Response surface methodology (RSM) is one of the tools of DOE and it is commonly used for manufacturing experiments. RSM has been chosen due its robustness and simplicity in use [6, 7, 15, and 17]. In the experimental study, a well-planned and designed experimental set-up was prepared and the experiments were conducted in the CAD/CAM departmental laboratory. The experimental set-up consists of several equipments in order to obtain proper conditions and to obtain reasonable results. In the followings, the design of experiments is explained in detail and the experimental set-up, procedure, equipments and tools are introduced.

3.2 Design of Experiment

Experiments are performed by investigators in virtually all fields of inquiry, usually to discover something about a particular process or system. We can define an experiment as a test or series of tests in which purposeful changes are made to the input variables of a process or system so that we may observe and identify the reasons for changes that may be observed in the output response. [21] In general usage, design of experiments or experimental design is the design of any information-gathering exercises where variation is present, whether under the full control of the experimenter or not. [21] Experimental design and methods have found

broad application in many disciplines. Experimental design is a critically important tool in the engineering world for improving the performance of manufacturing process. It also has extensive application in the development of new processes. The application of experimental design techniques early in process development can result in [21]:

- Improved process yields
- Reduced variability and closer conformance to nominal or target requirements
- Reduced development time
- Reduced overall costs

There are four tools of DOE: Factorial, RSM, Taguchi and Mixture. Taguchi and RSM are two of the commonly used DOE methods. There are some advantages and disadvantages between RSM and Taguchi methods; the major difficulty in analyzing results using these techniques is in the number of control factors and responses. The Taguchi analysis can provide definitive information if there is only one response but it does not deal very well with situations where a number of responses are to be optimized. Using RSM, only two control factors may be viewed at a time on a single contour plot although more than about four responses on one graph become very difficult to interpret. However, since a response surface is available an automatic optimizer can be used to help determine the optimum setting for each response. Constraints can be set on response values and the ability of define a composite response which encapsulates all of responses together makes multi-parameters response optimization simple. User-defined weighting can also be implemented if some requirements are deemed more important than others. This is all possible since RSM fits surface to data which enables interpolation at factor values in between those used for the simulations. [22]

In this work, there are four different input parameters (factors) and three different output parameters (responses) are correlated and the output parameters are optimized. Taguchi can only deal with one response, but RSM just only have this tool and ability to make automatic optimization with more than one response. Thus DOE and RSM were used to model the experiments to be conducted in this study.

The minimum number of experiments related to the number of inputs and outputs were also determined.

RSM was implemented using statistical software, MINITAB®. Before conducting the experiments, identification the process parameters and selecting proper machine settings were performed via preliminary experiments. In order to that, the prepared specimens were drilled with different process parameters (I, Ton, Toff, C, Vg) and dielectric fluid pressure Pr. In fact, all of these input parameters were effecting the results and some of them had more dominant effect on the output results. They were I, Ton, Toff and C. Vg caused to high over-cut which is not admitted in precise machining. The preliminary experimental results have shown that the Pr had no strong effect on the results.

The EDM drilling machine has ten different setting levels (0, 1, 2, 3, 4, 5, 6, 7, 8 and 9) for each chosen inputs. According to the preliminary experiments that were conducted for the same workpiece materials and the designed experimental conditions, levels from five to zero had no substantial effects on the material removal rates. In other words, there was almost no feed on the electrode. The holes could not been generated due to the insufficient MRR and therefore EWR and Ra had not measured. Thus, in the experimental design of this work, only five levels of settings (5, 6, 7, 8 and 9) were chosen. There are some output results which can be obtained from the experiments, such as MRR, EWR, Ra, overcut and white layer thickness etc. In this study, MRR, EWR and Ra are chosen as the responses [3, 4, 5, 6, 7, 9, 13, 15 and 16].

There are four different input parameters that are called as factors and each factor has five different machine settings (5 to 9). The software works with codes and the factors were converted to the codes. So, five different codes were generated for four factors. Codes can be selected with any of two different numbers, than the software find their median and their extrapolation and interpolation point. In this study, the factors were chosen from [-1 to 1] and the software derived the other codes between [-2 to 2]. These are [-2, -1, 0, 1, 2] to fit the five settings. For example, current maximum value was coded to 2 and current minimum value was coded to -2. Coded values for settings are given in Tables 3.1 and Table 3.2 shows the coded settings, which are given in their operational values.

Table 3.1 Coded factors of EDM hole drilling machine settings

Codes	**-2**	**-1**	**0**	**1**	**2**
Current (I)	5	6	7	8	9
Pulse on (Ton)	5	6	7	8	9
Pulse off (Toff)	5	6	7	8	9
Capacitance(C)	5	6	7	8	9

Table 3.2 Coded factors value

Codes	**-2**	**-1**	**0**	**1**	**2**
Current (A)	8,2	8,8	10,2	11,5	12
Ton (μs)	27	30	35	38	44
Toff (μs)	16	18	20	23	26
Capacitance (μF)	1100	1217	1316	1422	1476

In order to designate the factors of the real values, the machine catalogue was used. Ton, Toff and C were obtained from the machine producer catalogue. The catalogue of the producer does not give any information about discharge current and therefore current values were measured on EDM hole drilling machine by a special-purpose current probe (80i-110s AC/DC fluke current probe) via oscilloscope (Rigol R500) for each machine setting.

In order to generate the number of experiments to be conducted using RSM. Firstly, the response surface (RS) tool, which is one of the tools of DOE to create RS design in the software, was initiated. The central composite design (CCD) was selected due to its robustness and simplicity. The CCDs are most popular among the various classes of RSM designs due to its sequentially running, efficiency and flexibility [21].Thirty one (31) experiments were obtained by applying DOE using RSM. This number of experiments was conducted to each workpiece and electrode material combination. For instance, Ti64-copper electrode, Ti64-brass electrode, In718-copper electrode and In718-brass electrode. The coded values of the experiments with random order are depicted in Table 3.3. These coded 31 experiments were converted to the machine setting and are given in Table 3.4. Table 3.5 shows the exact machine setting values.

Table 3.3 Thirty one coded experiments

Std-Order	Run-Order	Pt-Type	Blocks	I(A)	Ton(µs)	Toff(µs)	C(µF)
25	1	0	1	0	0	-2	0
7	2	1	1	0	0	2	0
14	3	1	1	-1	-1	0	-1
16	4	1	1	0	0	0	0
26	5	0	1	-1	-1	-1	1
23	6	-1	1	-1	-1	1	1
19	7	-1	1	-2	0	0	0
28	8	0	1	1	1	-1	1
18	9	-1	1	1	1	-1	-1
10	10	1	1	-1	-1	-1	-1
27	11	0	1	1	1	1	-1
15	12	1	1	-1	1	-1	-1
31	13	0	1	0	0	0	0
8	14	1	1	1	-1	1	1
22	15	-1	1	0	0	0	2
29	16	0	1	0	0	0	-2
11	17	1	1	0	0	0	0
1	18	1	1	-1	1	1	1
9	19	1	1	0	0	0	0
4	20	1	1	-1	1	-1	1
6	21	1	1	1	-1	-1	1
24	22	-1	1	0	-2	0	0
21	23	-1	1	0	0	0	0
17	24	-1	1	0	0	0	0
13	25	1	1	2	0	0	0
20	26	-1	1	1	-1	1	-1
3	27	1	1	0	0	0	0
30	28	0	1	1	-1	-1	-1
12	29	1	1	0	2	0	0
5	30	1	1	1	1	1	1
2	31	1	1	-1	1	1	-1

Table 3.4 Thirty one experiments coded with EDM machine setting. The sequence shown in this table also was used in the conducted experiments.

Experiment #	Current (I)	Pulse on (Ton)	Pulse off (Toff)	Capacitance (C)
1	7	7	5	7
2	7	7	9	7
3	6	6	7	6
4	7	7	7	7
5	6	6	6	8
6	6	6	7	7
7	5	7	7	7
8	8	8	6	8
9	8	8	6	6
10	6	6	6	6
11	8	8	8	6
12	6	8	6	6
13	7	7	7	7
14	8	6	8	8
15	7	7	7	9
16	7	7	7	5
17	7	7	7	7
18	6	8	8	8
19	7	7	7	7
20	6	8	6	8
21	8	6	6	8
22	7	5	7	7
23	7	7	7	7
24	7	7	7	7
25	9	7	7	7
26	8	6	8	6
27	7	7	7	7
28	8	6	6	6
29	7	9	7	7
30	8	8	8	8
31	6	8	8	6

Table 3.5 Thirty one experiments with their exact values

Experiment #	Current(A)	Pulse on(µs)	Pulse off(µs)	Capacitance(µF)
1	10,2	35	16	1316
2	10,2	35	26	1316
3	8,8	30	20	1217
4	10,2	35	20	1316
5	8,8	30	18	1422
6	8,8	30	20	1316
7	8,2	35	20	1316
8	11,5	38	18	1422
9	11,5	38	18	1217
10	8,8	30	18	1217
11	11,5	38	23	1217
12	8,8	38	18	1217
13	10,2	35	20	1316
14	11,5	30	23	1422
15	10,2	35	20	1476
16	10,2	35	20	1100
17	10,2	35	20	1316
18	8,8	38	23	1422
19	10,2	35	20	1316
20	8,8	38	18	1422
21	11,5	30	18	1422
22	10,2	27	20	1316
23	10,2	35	20	1316
24	10,2	35	20	1316
25	12	35	20	1316
26	11,5	30	23	1217
27	10,2	35	20	1316
28	11,5	30	18	1217
29	10,2	44	20	1316
30	11,5	38	23	1422
31	8,8	38	23	1217

3.3 Experimental procedure and set-up

In this study, two different materials (Inconel 718 and Ti-6Al-4V) were used as the work-piece materials. These materials are in fact alloys of nickel and titanium materials which are commonly used for manufacturing of turbines and jet engine components. The EDM hole drilling operations were conducted using with two different types of electrode materials: brass and copper. These electrode materials are

popular and commonly used in EDM hole drilling operations, particularly for aerospace alloys. [15-16]. Drilled hole diameters may vary from micro to macro scale. EDM micro hole drilling reaches to 50µm diameter holes. [15-16] In this work, the drilled holes were limited between 0,4 to 3mm diameters [0.4, 0.5, 0.6, 0.7, 0.8, 0.9, 1, 1.5, 2, 2,5, 3]. Although 0.2 and 0.3mm diameter electrodes are available and planned to be drilled in the beginning of the experiments, the current EDM settings failed with these diameters. In fact, 0.2 and 0.3mm electrodes were used in the preliminary experiments and the electrodes were cut-off during the drilling operations.

Using of two types of workpiece and electrode materials and eleven different diameters produced 1364 experiments to be conducted. Thus, each material is drilled in 11 different diameters with each electrode material. Figure 3.1

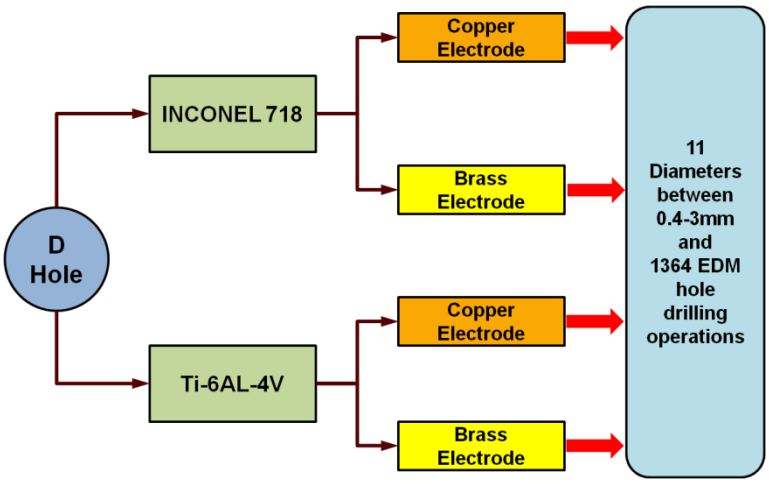

Figure 3.1 Schematic view of experiments

3.3.1 Machine and equipments

JS AD-20 EDM was used as the EDM hole drilling machine in the conducted experiments. Although this machine is typically used for drilling starting holes for wire EDM operations, it can also be used for hole drilling operations. The schematic representation and the picture of the machine are shown in Figure 3.2.

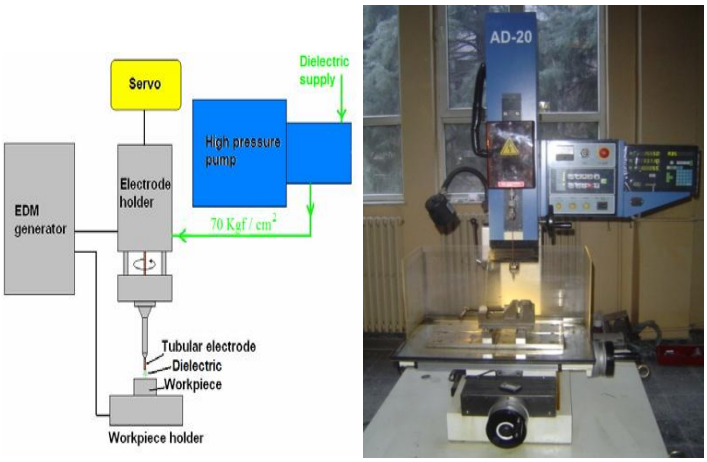

(a) (b)

Figure 3.2 (a) Schematic view of EDM Hole Drilling machine (b) Overall picture of EDM Hole Drilling machine

The EDM hole drilling machine has 3-axes (x-y-z). X and Y axes are positioned manually to move the table and the work-piece. Z-axis is controlled from the control unit via servo motor. Each axis is also monitored with an electronic axis pointer in order to obtain precise positioning. The machine has a vertical head consisting of servo mechanism, mandrel, ceramic guide unit and dielectric pumping unit. The electrode is mounted to the mandrel and rotated via electric motor assembled to the vertical head. Vertical movement of the electrode is supplied by the servo motor and mechanism. In order to have precise rotation and prevent bending during drilling, a ceramic guider and its units are assembled on the vertical head. Dielectric water is pumped from a reservoir via pipes and directed to inside the electrode.

The control unit of the machine consists of voltage control, servo control and speed control. The voltage level can be set to three levels (V0, V1 and V2). The experiments were conducted at V1. Servo and speed control switches are used for changing the servo and vertical linear movement speed of the head. The EDM process parameters (I, Ton, Toff and C) can also be controlled from the machine control unit. To do that, each parameter is set to a number from 0 to 9 by pressing the buttons. The settings are leveled from minimum to maximum value and working in combination with the voltage level. The picture of the head and the control unit are shown in Figure 3.3

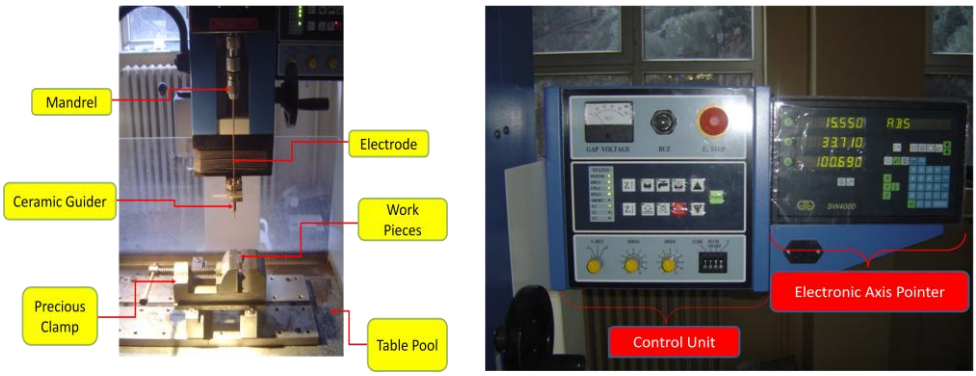

Figure 3.3 (a) Overall picture and (b) Control Unit of JS AD-20 EDM

Although the EDM drilling machine has working table and simple vise, a precise vise was used in the experiments. In order to clamp the workpieces in a simply manner and obtain error-free positioning, a three-contact-point fixture was designed that can be mounted to the precious vise, as shown in Figure 3.4.

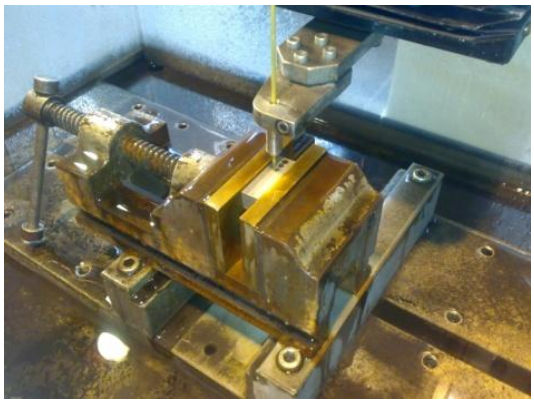

Figure 3.4 Precious vise and special fixture

Deionized (DI) water was used as dielectric fluid in the experiments. DI is a poor conductor but it is a good insulator. During discharge, a large enough electrical potential can cause the fluid to break down into ionic (charged) fragments which allows an electrical current to pass from the electrode to the workpiece [1]. High pressure pump is pumping the DI water through the electrode channel onto work pieces. DI water stabilizes the discharge and flashed away the debris from drilling area. High pressure DI water cools the electrode and workpiece as well as makes the electrode stiff while rotating in its axis.

High precious scale was used for measuring weight differences of the workpieces before and after drilling operations. MRR are calculated using with these weight differences over time. Precision of the scale is 0.001 gr.

An electronic timer is used to determine the time (sec) during the experiments. The drilling time for each hole was recorded using this electronic timer.
After drilling of the work pieces, the drilled surfaces were analyzed and surface roughness of these surfaces were measured. Drilled surfaces were firstly analyzed by a scanning electron microscope (SEM), JEOL JSM 6390LV. The drilled surfaces were captured at different magnification and orientations. These captures were then analyzed via an optical measurement and inspection software (Alicona MeX®). The analyses were based on measuring hole diameters, extracting holes profiles and measuring surface roughness.

3.3.2 Test pieces

The work piece materials used in this study are common aerospace super alloys: Inconel 718 (IN718) and α+β type Ti-6Al-4V (Ti64). In spite of poor machinability and low mechanical properties, these materials are preferred in aerospace applications due to their specific thermal and physical properties. Test pieces were prepared with the dimensions of 6 mm x 11 mm x 35 mm. These dimensions were deliberately chosen considering with the SEM limitations. Before conducting the experiments, the top, bottom and overlap surfaces of the work pieces were ground and polished with a surface grinding machine. The overlap surfaces of the two specimens were sticked together with a precise adjustment. The holes were drilled along the intersection line of the two pieces, as shown in Figure 3.5. The chemical compositions and properties of Inconel 718 and Ti-6Al-4V alloys are given in Tables 3.6-3.9.

Table 3.6 Chemical composition of Inconel 718 (wt. %)

Ni	50-55	Al	0.20-0.80
Cr	17-21	Si	0.35 max
Fe	Balanced	Mn	0.35 max
Nb(+Ta)	4.75-5.50	Cu	0.30 max
Mo	2,80-3.30	C	0.08 max
Co	1.00 max.	B	0.06 max
Ti	0.65-1.15		

Table 3.7 Chemical composition of Ti6Al4V (wt. %)

Ti	89.464	O	0.18
Al	6.08	C	0.02
V	4.22	N	0.01
Fe	0.22	H	0.0053

Table 3.8 Properties of Inconel 718

Density	Kg/cu m	8220
Electrical Resistivity	microhm-mm	1210
Melting point	°C	1210-1344
Modulus of elasticity	GPa	208
Tensile strength	Mpa	1407
%0.2 yield strength	Mpa	1172
Thermal conductivity	W/m- ºK	11.4

Table 3.9 Properties of Ti6Al4V

Density	kg/cu m	4430
Electrical Resistivity	microhm-mm	1780
Melting point	°C	1604
Modulus of elasticity	GPa	113.8
Tensile strength	Mpa	950
%0.2 yield strength	Mpa	880
Thermal conductivity	W/m- ºK	7.2

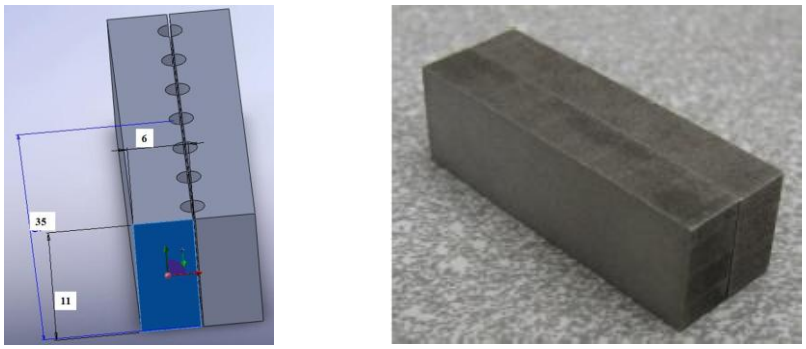

Figure 3.5 Dimensions of the work pieces and demonstration of the holes in a solid model

3.3.3 Electrodes

Two different types of electrode materials were used in the experiments. Brass and copper are the material types of the electrode and single-channel exists inside the electrodes, since the electrodes are hollow in order to pumping dielectric fluid through it, as shown in Figure 3.7. Brass and copper have different properties and used for different purposes in EDM operations. The main factor of choosing these materials as electrode materials is their high electrical conductivity and cheapness. The major properties of these materials are given in Table 3.10.

Table 3.10 Major properties of electrode materials

Electrode Material	**Copper**	**Brass**
Melting point (^{0}C)	1084.62	900-940
Electrical resistivity (ohm-cm)	1.69	4.70
Thermal conductivity (W/m-^{0}K)	391	159
Specific heat capacity (J/g-^{0}C)	0.385	0.380

Figure 3.6 Single-channel (a) brass (b) copper electrodes

3.3.4 Experimental Procedure

The experiments were conducted in the departmental laboratories and equipments. The experiments were conducted in a random order so as to remove the effects of any unaccounted factors, such as heat effects, dirt effects on electrodes etc. RSM produced 31 experiments and repeated five of these experiments [7, 7, 7, 7] in order to find the reproducibility. The reproducibility is used to determine the variability in measurements due to operators and the operator-part interaction. Before drilling of each hole, the workpieces were weighted, precisely clamped and the electrode was positioned correctly. The experiments were conducted using with the variable settings and constant settings which are given in Table 3.11. After drilling of the through holes, the pieces were washed, dried and weighted again. The completion of a hole was signalled by the emergence of the dielectric jet through the bottom of work-piece. The time elapsed was also measured. The measurements covered the weight, the time for drilling, the electrode length, the rest of the measurements (MRR, EWR, Ra) were performed via calculations and image processing.

In the experiments, considerable amount of holes were drilled and therefore a code system was established to designate the holes drilled on the workpieces. This designation shows the hole diameter, materials type, electrode used, and the order of the experiments. For instance, D2NiBr 9-10-11 designates the holes drilled with the 9^{th}, 10^{th} and 11^{th} order of the experiments with 2 mm diameter brass electrodes on Inconel 718.

Table 3.11 Experimental variables and constants

Experimental variables	**Variance**	**Machine Settings**
Discharge Current,I (A)	10-30	1-9
Pulse on, T_{on} (µs)	8-44	1-9
Pulse off, T_{off} (µs)	5-26	1-9
Capacitance, C (µF)	104-1422	1-9
Experimental constants		
Voltage (Volt), V1	27	
Dielectric fluid	Deionized Water	
Dielectric pumping pressure (bar)	75	
Electrode revolution speed (rpm)	150	
Electrode polarity	(-) Nagative	

3.4 Experimental Measurements

3.4.1 Material Removal Rate (MRR)

The specimens were weighted before and after drilling operations using an accurate digital weighing machine. The EDM hole drilling time was recorded for each hole via an electronic timer. The material removal rate was calculated using the following formula:

$$\text{MRR}=\frac{\text{İ}nitial\ \ Weig\,ht-Final\ \ Weig\,ht}{Mac\,hining\ \ Time}\ gram/min \qquad 3.1$$

3.4.2 Electrode Ware Rate (EWR)

The amount of electrode consumed for each drilled hole was measured using the digital axis control panel of the EDM fast hole drilling machine. Electrode was contacted two times with work-pieces. Before drilling, the electrode was contacted the top surface of the pieces and the digital axis set to zero in z-axis. After drilling, the electrode was touched to the top surface of the work-piece again and the difference in length (mm) between first and second touches is shown on digital panel

as numerical value, which was taken as the electrode loss in length. Then EWR is calculated as follows:

$$\text{EWR}=\frac{Consumed\ \ Electrode\ \ in\ Length}{Machining\ \ Time}\ mm/min \qquad 3.2$$

3.4.3 Surface Roughness (Ra)

Surface roughness measurements are necessary to understand the quality of the drilled surfaces after operations. In order to measure the surface roughness of the drilled holes in this work, an image processing based surface roughness measurement technique and the dedicated software (Alicona MeX®) were used. The holes drilled in this work are varying between 0.4 to 3 mm in diameter. These holes have cylindrical surfaces and the half of the pieces is used in the measurements. Stylus type contact surface roughness measurement techniques were tested for the measurements. In these preliminary tests, it was able to measure large diameters (3, 2.5, and 2mm) since a small stylus was available. But, however, for small diameters less than 1 mm, it was not able to measure since there is no stylus to fit such small areas. Therefore, the dedicated software which is based on 3D measurements using scanning electron microscope images was used. It allows fully topographic examinations, such as surface, profile, roughness, area and volume, using high quality images from SEM.

The image formation process in the SEM is based on perspective projection. Similar to a conventional light microscope the three dimensional object is projected onto a two dimensional image plane and information about the third dimension is lost. Note, the large depth of focus in SEM provides full depth of focus images, but does not allow to measure depth. Only two dimensional measurements in the image plane are feasible. An eccentric tilting of the stage, meaning that the intersection of the primary electron beam with the specimen define the centre of tilting, yield a second image of the specimen observed form a different viewpoint. In the measurements, the one half of the workpieces was selected to be examined in the SEM. This piece was then located SEM examination table precisely and the images were taken with the desired magnifications. In order to obtain the full image of the holes, x8, x9, and x10 magnifications were used depends on the hole diameters. In the image analyses, the profile, area and volume can be performed, therefore the depth of the images should

also be captured. To do that, two images were captured with different orientations. One was captured when the table was in zero tilting angle and the other was captured with tilting angles which was +5 or +10 depends on the hole sizes. Thus, two images were obtained from a workpiece, as shown in Figure 3.7.

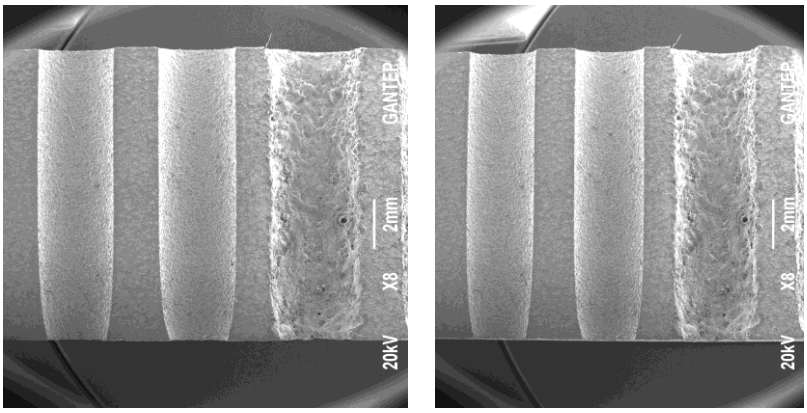

(a) (b)

Figure 3.7 SEM images (a) D2NiBr 9-10-11x8 ve (b) D2NiBr 9-10-11x8+10deg with x8 magnification and +10deg tilting

The captured images were merged and a surface model was generated. Depending on the quality and the surface similarities of the drilled hole surfaces, two or three images were used to generate surface models, as shown in Figure 3.8.

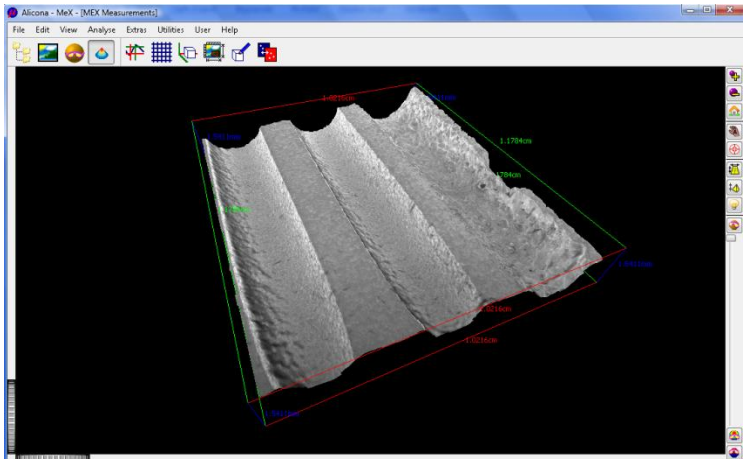

Figure 3.8 A 3D surface model generated from captured SEM images

The generated 3D surfaces allow analyzing profile, area and volume of the drilled holes, as well as some dimensional measurements could be performed, such as the diameter, length, angle etc. In this work, some dimensional measurements and the surface roughness were measured from 3D surfaces.

Surface roughness measurements were based on ISO 4287 and 4288 standards using with 0.8 cut-off length. Average roughness (Ra) was regarded in the measurements. Three measurements were taken from a hole surface: entrance, middle and exit. Then the average of these three values was accepted as the hole surface roughness values. Figure 3.9 and 10 depict the roughness measurements.

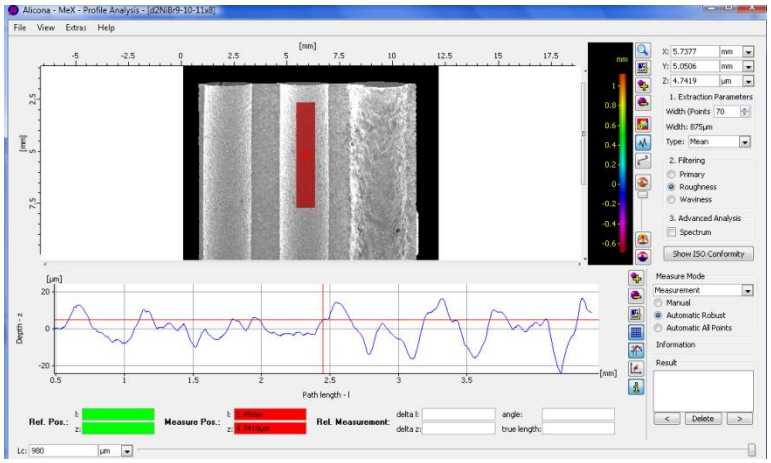

Figure 3.9 Surface roughness (Ra) measurement

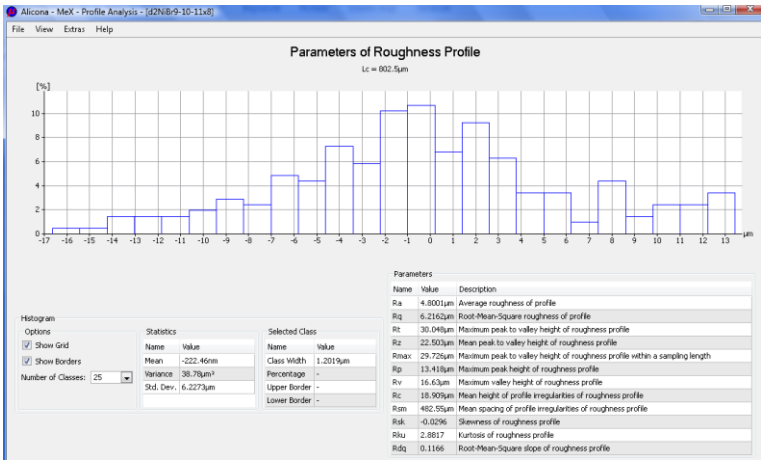

Figure 3.10 Roughness results

Moreover, the profile of the drilled hole surfaces and the dimensions were measured. In these measurements, the profiles were used to investigate the semi-cylindrical shape of the holes. Linear measurements were made to find the diametric changes of the holes. Figures 3.11 and 3.12 show these measurements. The experiments have also showed that an overcut is occurred with the following condition:

Over-cut =Electrode diameter x 0.1 3.3

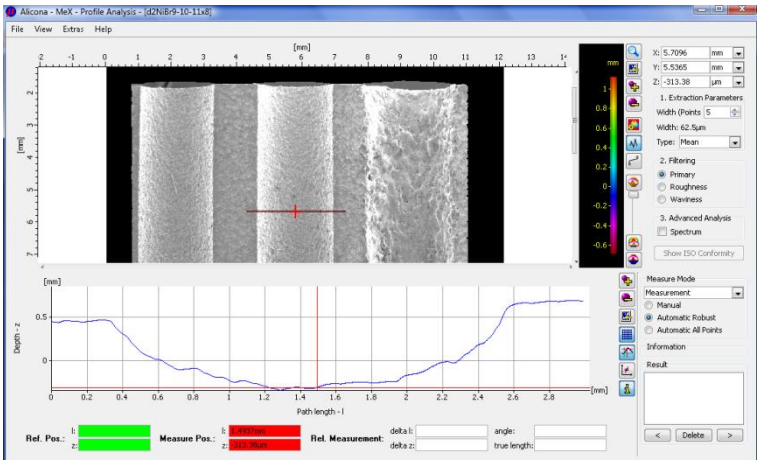

Figure 3.11 Profile analysis

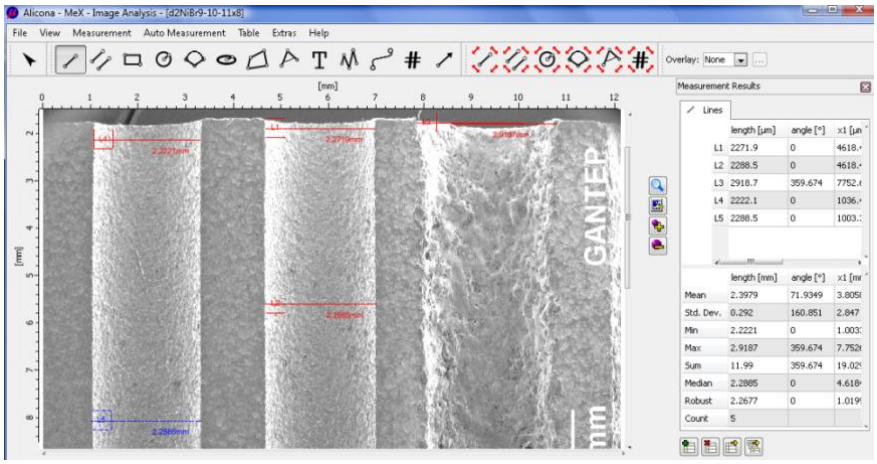

Figure 3.12 Linear measurements

CHAPTER 4

MODELLING AND OPTIMISATION OF THE EDM FAST HOLE DRILLING OPERATIONS

4.1 Introduction

This research work covers a considerable amount of experiments in order to investigate the EDM fast hole drilling characteristics for Inconel 718 and Ti-6Al-4V alloys. This investigation comprises conducting experiments, designing and modelling of the experiments using Response Surface Methodology, mathematical modelling, obtaining main effects and interaction plots and optimisations. This chapter consists of the methodology and procedure that were developed and followed while doing the necessary investigations for EDM fast hole drilling processes. Firstly, the experimental results obtained from the conducted experiments are given in the tables. These data were then used to generate mathematical models using RSM and ANOVA techniques. Using the mathematical models, the predicted results were calculated and tabulated. The percentage errors between these results are also depicted in the tables. The effects of the inputs to the EDM outputs are then discussed and interaction graphs are also shown. Optimisation of the EDM settings is of primary objective in this work and the methodology followed and the optimum results are also included in this chapter. Finally, a validation experimental design was developed and implemented in order to evaluate the mathematical models.

In this research works, 11 different diameters (0,4-3mm), two different alloys (Inconel 718 and Ti-6al-4V) and two different electrode materials (brass and copper) were used in the investigations. Therefore, there are plenty of data, graphs, tables and empirical equations which were obtained throughout this research work. Instead of presenting all these information in this thesis, only selected results are discussed and the developed methodology is explained as an example. The rest of the results found are shown in the tables. Thus, ∅2mm holes drilled with brass and copper electrodes

on Inconel 718 (D2NiBr & D2NiCu) and Ti-6Al-4V (D2TiBr & D2TiCu) was chosen as a sample application.

4.2 Experimental Results of EDM fast hole drilling operations

Experimental results of MRR, EWR and Ra were obtained for the input parameters. In Tables 4.1, 4.2, 4.3 and 4.4 shows these results for D2NiBr, D2NiCu, D2TiBr and D2TiCu.

Table 4.1 Experimental results of MRR, EWR and Ra for D2NiBr

Exp. No	I (A)	Ton (µs)	Toff (µs)	C (µF)	Exp_MRR (gr/min)	Exp_EWR (mm/min)	Exp_Ra (µm)
1	6	6	6	6	0,062	0,384	10,941
2	7	7	5	7	0,093	0,866	12,054
3	8	8	8	8	0,128	1,825	3,982
4	8	6	8	8	0,107	1,655	3,771
5	7	7	7	7	0,081	0,814	12,809
6	7	7	7	7	0,080	0,722	11,608
7	7	7	7	7	0,079	0,702	12,305
8	7	7	7	9	0,104	1,341	3,858
9	8	8	6	8	0,136	2,118	3,863
10	6	8	6	8	0,119	1,612	4,357
11	6	6	8	6	0,069	0,701	11,483
12	7	7	7	7	0,089	0,814	10,513
13	6	8	8	8	0,118	1,498	4,037
14	8	6	8	6	0,083	0,779	12,086
15	8	8	6	6	0,102	0,827	10,659
16	9	7	7	7	0,147	1,962	3,545
17	6	8	6	6	0,089	0,742	10,630
18	6	6	6	8	0,093	1,194	4,672
19	7	7	9	7	0,081	0,941	10,690
20	7	9	7	7	0,103	0,930	11,728
21	8	6	6	6	0,094	0,822	12,277
22	7	7	7	7	0,088	0,736	10,462
23	7	7	7	7	0,084	0,736	11,592
24	7	5	7	7	0,075	0,623	10,312
25	6	8	8	6	0,082	0,675	11,633
26	8	8	8	6	0,096	0,870	11,871
27	6	6	8	8	0,094	1,219	3,810
28	8	6	6	8	0,114	1,812	4,447
29	5	7	7	7	0,063	0,611	11,105
30	7	7	7	5	0,085	0,850	10,767
31	7	7	7	7	0,074	0,576	10,005

Table 4.2 Experimental Results of MRR, EWR and Ra for 2mm D2NiCu

Exp. No	I (A)	Ton (µs)	Toff (µs)	C (µF)	Exp_MRR (gr/min)	Exp_EWR (mm/min)	Exp_Ra (µm)
1	6	6	6	6	0,048	0,205	11,425
2	7	7	5	7	0,054	0,379	10,199
3	8	8	8	8	0,082	1,476	4,054
4	8	6	8	8	0,067	1,204	4,018
5	7	7	7	7	0,050	0,461	9,565
6	7	7	7	7	0,053	0,495	10,211
7	7	7	7	7	0,052	0,507	9,733
8	7	7	7	9	0,065	0,963	4,118
9	8	8	6	8	0,080	1,374	4,139
10	6	8	6	8	0,075	1,009	3,626
11	6	6	8	6	0,038	0,317	11,549
12	7	7	7	7	0,052	0,634	10,480
13	6	8	8	8	0,065	0,726	3,479
14	8	6	8	6	0,048	0,354	12,869
15	8	8	6	6	0,059	0,450	11,756
16	9	7	7	7	0,083	1,035	3,880
17	6	8	6	6	0,057	0,419	10,946
18	6	6	6	8	0,059	0,548	3,692
19	7	7	9	7	0,054	0,631	9,608
20	7	9	7	7	0,061	0,566	9,663
21	8	6	6	6	0,063	0,599	12,214
22	7	7	7	7	0,060	0,590	8,999
23	7	7	7	7	0,058	0,550	9,369
24	7	5	7	7	0,054	0,667	9,277
25	6	8	8	6	0,053	0,492	11,712
26	8	8	8	6	0,056	0,281	11,831
27	6	6	8	8	0,066	1,006	4,104
28	8	6	6	8	0,059	0,894	3,841
29	5	7	7	7	0,036	0,189	9,164
30	7	7	7	5	0,050	0,410	9,160
31	7	7	7	7	0,058	0,727	9,399

Table 4.3 Experimental Results of MRR, EWR and Ra for D2TiBr

Exp. No	I (A)	Ton (µs)	Toff (µs)	C (µF)	Exp_MRR (gr/min)	Exp_EWR (mm/min)	Exp_Ra (µm)
1	6	6	6	6	0,058	0,282	10,306
2	7	7	5	7	0,062	0,438	12,043
3	8	8	8	8	0,094	0,950	4,628
4	8	6	8	8	0,077	0,666	3,724
5	7	7	7	7	0,035	0,189	11,670
6	7	7	7	7	0,044	0,218	12,056
7	7	7	7	7	0,050	0,303	11,476
8	7	7	7	9	0,071	0,613	3,940
9	8	8	6	8	0,068	0,712	3,699
10	6	8	6	8	0,075	0,659	3,952
11	6	6	8	6	0,047	0,157	11,254
12	7	7	7	7	0,046	0,201	11,363
13	6	8	8	8	0,072	0,515	4,161
14	8	6	8	6	0,040	0,217	12,894
15	8	8	6	6	0,048	0,260	12,096
16	9	7	7	7	0,071	0,547	9,959
17	6	8	6	6	0,059	0,273	11,337
18	6	6	6	8	0,061	0,489	4,047
19	7	7	9	7	0,050	0,369	12,152
20	7	9	7	7	0,065	0,431	12,691
21	8	6	6	6	0,062	0,324	12,692
22	7	7	7	7	0,056	0,317	12,350
23	7	7	7	7	0,055	0,323	13,978
24	7	5	7	7	0,051	0,251	11,143
25	6	8	8	6	0,060	0,338	11,316
26	8	8	8	6	0,062	0,188	11,153
27	6	6	8	8	0,053	0,360	3,940
28	8	6	6	8	0,064	0,600	3,518
29	5	7	7	7	0,042	0,218	11,650
30	7	7	7	5	0,058	0,311	10,113
31	7	7	7	7	0,059	0,328	10,917

Table 4.4 Experimental Results of MRR, EWR and Ra for D2TiCu

Exp. No	I (A)	Ton (µs)	Toff (µs)	C (µF)	Exp_MRR (gr/min)	Exp_EWR (mm/min)	Exp_Ra (µm)
1	6	6	6	6	0,053	0,129	11,502
2	7	7	5	7	0,043	0,105	11,133
3	8	8	8	8	0,050	0,146	4,426
4	8	6	8	8	0,060	0,214	4,337
5	7	7	7	7	0,036	0,062	10,601
6	7	7	7	7	0,036	0,066	9,715
7	7	7	7	7	0,035	0,096	10,753
8	7	7	7	9	0,061	0,295	4,047
9	8	8	6	8	0,086	0,455	3,221
10	6	8	6	8	0,030	0,069	4,566
11	6	6	8	6	0,029	0,041	12,518
12	7	7	7	7	0,028	0,050	11,077
13	6	8	8	8	0,045	0,180	4,356
14	8	6	8	6	0,033	0,068	13,775
15	8	8	6	6	0,046	0,099	10,305
16	9	7	7	7	0,079	0,235	3,828
17	6	8	6	6	0,030	0,062	10,517
18	6	6	6	8	0,050	0,306	3,204
19	7	7	9	7	0,030	0,054	9,753
20	7	9	7	7	0,034	0,083	10,461
21	8	6	6	6	0,041	0,130	10,717
22	7	7	7	7	0,034	0,099	10,490
23	7	7	7	7	0,034	0,102	10,453
24	7	5	7	7	0,027	0,085	11,210
25	6	8	8	6	0,033	0,087	10,713
26	8	8	8	6	0,039	0,132	11,737
27	6	6	8	8	0,031	0,170	4,256
28	8	6	6	8	0,049	0,386	4,306
29	5	7	7	7	0,029	0,060	11,407
30	7	7	7	5	0,026	0,041	11,472
31	7	7	7	7	0,035	0,083	11,403

When the work pieces were drilled by brass electrodes, there are some differences in responses observed on the repeated experiments. Experimental errors may cause these differences. Measurement errors could cause these errors either. On the other hand, EDM machining is a very sophisticated process and the method has different effective factors which have strong effect on the process. Some of the factors can be kept under control but many of them cannot. However, RSM uses a strategy that the repeated measurements are considered as their average values.

4.3 Mathematical modelling of EDM fast hole drilling process

4.3.1 Response Surface Methodology

Response surface methodology (RSM) is a collection of mathematical and statistical techniques that are useful for modelling and analysis of problems in which output or response influenced by several variables and the goal is to find the correlation between the response and the variables. The final objective is to optimize the responses. The variables that influence the behaviour of the system are called factors. If all the input parameters represent quantitative variables then the responses can be represented as a function of levels and variables.

$$Yu = f(X_{1u}, X_{2u}, \ldots . X_{ku}) + E_u \qquad \textbf{4.1}$$

Where, u=1, 2...N represents N observation in the factorial experiment and X_{iu} represents the level of i^{th} factor in u^{th} observation. The function 'f' is called the response function. The residual E_u measures the experimental error of the u^{th} observation.

In the present experimental investigation, the effects of EDM conditions such as discharge current (I), pulse on time (Ton), pulse off time (Toff) and capacitance (C) on MRR, EWR and Ra were studied. The design of experiments was stated in the previous chapter. Since the EDM process is non-linear in nature, the linear polynomial will not be able to predict the responses accurately. Therefore, in this work a second-order polynomial (quadratic model) was used for developing the empirical model relating the response surface and independent parameters as shown below [16].

$$Y = b_0 + \sum_{i=l}^{k} b_i\, x_i + \sum_{i=l}^{k} b_{ii}\, x_{iu}^2 + \sum_{i<l=2}^{k} b_{ij}\, x_{iu} x_{ju} \qquad \textbf{4.2}$$

The response surface methodology was then applied and the mathematical relation for correlating the MRR, EWR and Ra and the considered process variables were obtained. These equations include outputs, constant values and input parameters and their coefficients. Input parameters were used as coded values. Therefore the generated mathematical models had to be used as coded. The input variables were coded between [5 to 9] in the mathematical relations. However, outputs were obtained in their real values as MRR (gr/min), EWR (mm/min) and Ra (□ m). Real

values of the input parameters had to be changed to coded parameters. Therefore, linear and exponential functions were generated to provide necessary transformations. Linear functions can convert real values to the coded values without using a range but the exponential functions can only convert real values to the coded values in a given range. Table 4.5 shows these functions and the ranges. Mathematical relation for correlating the MRR, EWR and Ra for D2NiBr is given in Table 4.6. The rest of the mathematical relations were generated for all diameters and the materials, but they are not given in a form of mathematical equations. The rest of the empirical equations are given in a tabulated form which gives the coefficients and the sign of the effects of the process variables. These response equations can be obtained from Table 4.7 to 4.18.

Table 4.5 Linear and exponential functions

Input Parameters	Linear Function	Exponential Function
8.2 ≤ I (A) ≤ 12	0.9474*I – 2,6065	0.1742*I³ – 5,2615*I² + 53.409* I – 175,2
27 ≤ Ton (µs) ≤ 44	0.2349* Ton – 1,1745	– 0.0038*Ton² + 0,5048* Ton – 5,8189
16 ≤ Toff (µs) ≤ 26	0.3956* Toff – 1,1487	– 0.0137*Toff² + 0,9704* Toff – 7,0217
1100 ≤ C (µF) ≤ 1476	0.0103* C – 6,4683	9E-6*C² - 0,0123* C +7.952

Table 4.6 Response equations for D2NiBr

MRR=	471,989-50,105(I)-25,064(Ton)-13,223(Toff)-53,291(C)+6,615(I^2) +2,650(Ton^2)+2,118($Toff^2$)+3,889(C^2)-1,591(I*Ton)-1,997(I*Toff)-0,680(I*C)-0,835 (Ton*Toff)+1,952(Ton*C)+0,163(Toff*C)
EWR=	13.500- 2.101 I- 0.313 Ton- 0.117 Toff – 1.767 C+ 0.165 I² + 0.038 Ton^2 + 0.070 Toff²+ 0.118 C^2- 0.029 I*Ton- 0.038 I*Toff + 0.068 I*C- 0.036 Ton*Toff+0.047 Ton*C- 0.049 Toff*C
Ra=	-126.334 + 19.012 I- 3.319 Ton + 3.646 Toff + 17.009 C – 1.247 I² - 0.323 Ton^2 - 0.235 Toff² - 1.250 C^2- 0.122 I*Ton+ 0.06 I*Toff - 0.189 I*C + 0.2 Ton*Toff +0.096 Ton*C- 0.269 Toff*C

Table 4.7 Mathematical Models of In718-Brass MRR

NiBr	3mm	2,5mm	2mm	1,5mm	1mm	0,9mm	0,8mm	0,7mm	0,6mm	0,5mm	0,4mm
MRR=	MRR=	MRR=	MRR=	MRR=	MRR=	MRR=	MRR=	MRR=	MRR=	MRR=	MRR=
Constan	86,727	102,280	471,989	603,331	923,593	1649,700	1141,680	2263,280	374,361	59,444	533,848
I	18,930	14,745	-50,105	-49,942	-63,901	-259,760	-117,160	-277,630	-100,902	8,920	-11,589
Ton	17,525	9,440	-25,064	-31,156	-79,668	-52,880	-60,270	-137,320	35,587	-10,722	-56,258
Toff	-8,050	-2,598	-13,223	-28,593	-39,319	-28,630	-28,790	-91,870	-1,954	-14,213	-50,998
C	4,290	12,280	-53,291	-67,640	-97,866	-170,350	-146,560	-175,950	-51,819	-1,210	-41,382
I²	3,472	-0,008	6,615	7,168	3,153	14,620	7,380	11,660	5,334	2,006	0,076
Ton²	-0,996	-2,923	2,650	2,531	2,585	1,630	2,300	3,600	2,683	3,072	0,632
Toff²	0,220	-1,948	2,118	1,583	2,683	3,220	1,420	3,230	4,033	2,932	-0,206
C²	4,777	-0,531	3,889	6,631	7,977	13,260	9,430	9,250	6,061	7,874	1,685
I*Ton	7,296	1,794	-1,591	-1,031	0,236	4,190	0,730	6,800	-1,973	5,380	-1,685
I*Toff	2,811	-3,808	-1,997	-1,070	1,570	2,340	-0,070	4,170	1,401	-3,657	3,684
I*C	4,520	3,881	-0,680	-3,916	1,294	3,110	2,140	6,940	5,519	-7,810	-0,274
Ton*To:	-4,111	-1,694	-0,835	0,440	2,439	-2,010	0,750	2,590	-5,265	-2,825	4,647
Ton*C	5,555	1,157	1,952	0,709	3,866	2,360	2,950	3,550	-3,151	-7,976	4,327
Toff*C	-3,480	0,669	0,163	1,331	-4,006	-2,850	0,450	-0,250	-5,037	2,536	-0,522

Table 4.8 Mathematical Models of IN718-Copper MRR

NiCu	3mm	2,5mm	2mm	1,5mm	1mm	0,9mm	0,8mm	0,7mm	0,6mm	0,5mm	0,4mm
MRR=	MRR=	MRR=	MRR=	MRR=	MRR=	MRR=	MRR=	MRR=	MRR=	MRR=	MRR=
Constan	72,880	64,000	366,580	197,564	578,867	360,240	430,141	571,114	222,297	333,370	380,553
I	8,215	7,769	-20,447	-26,936	-65,095	-85,466	-9,757	-6,520	10,364	-20,007	-26,238
Ton	5,494	4,855	-22,101	2,601	-45,371	26,932	2,711	-26,243	-1,580	-18,254	-36,297
Toff	-2,484	-1,188	-25,953	-35,566	-18,244	37,482	14,590	3,161	-48,801	-13,078	-3,294
C	3,937	5,009	-36,161	10,630	-45,068	-95,332	-138,910	-145,233	-29,342	-50,410	-50,489
I²	-3,983	1,508	1,773	2,413	5,077	2,794	2,532	-0,036	-1,204	2,774	0,527
Ton²	-0,424	1,095	1,330	0,768	1,217	-3,216	-1,162	-1,229	0,025	1,693	1,411
Toff²	0,260	-0,310	0,452	1,744	1,925	-3,372	-1,009	-1,097	0,016	1,436	1,361
C²	-0,295	1,600	1,334	2,110	2,825	1,647	6,001	3,920	-0,944	4,147	3,186
I*Ton	1,889	2,975	-0,044	0,701	0,824	0,004	-2,943	-1,678	-2,149	-1,471	2,633
I*Toff	-0,681	-2,827	0,632	1,069	0,657	2,138	-2,160	-0,221	1,105	-0,704	-0,839
I*C	1,806	-2,231	-0,338	-1,983	-1,925	5,540	2,286	3,499	2,419	-0,411	1,095
Ton*To:	1,221	-0,824	-0,336	0,723	-1,058	-1,761	0,003	0,020	2,141	-0,046	-1,038
Ton*C	-1,521	1,766	1,434	-2,926	4,985	5,164	5,067	8,474	0,304	0,932	0,767
Toff*C	-0,354	2,914	2,352	-0,687	-1,080	1,137	1,882	2,136	4,059	-0,407	-0,161

Table 4.9 Mathematical Models of Ti64-Brass MRR

TiBr	3mm	2,5mm	2mm	1,5mm	1mm	0,9mm	0,8mm	0,7mm	0,6mm	0,5mm	0,4mm
MRR=	MRR=	MRR=	MRR=	MRR=	MRR=	MRR=	MRR=	MRR=	MRR=	MRR=	MRR=
Constan	80,404	56,540	1259,070	412,451	590,680	492,608	258,839	111,216	-71,9778	-210,74	13,6802
I	10,577	9,711	-71,150	-51,369	-36,694	37,845	-18,162	-0,357	4,0277	14,652	35,015
Ton	5,293	5,565	-70,920	-14,516	-30,687	-6,715	-3,394	-5,149	11,6348	36,695	-18,144
Toff	-2,699	0,039	-104,850	-20,364	-47,944	-7,762	-26,481	-8,472	-0,1581	-5,161	12,6506
C	7,035	10,611	-112,470	-34,413	-61,605	-175,042	-23,825	-16,31	6,7363	24,239	-38,2898
I²	2,951	8,076	2,470	3,411	1,678	-0,508	0,711	0,05	0,4651	-0,284	0,523
Ton²	-1,352	-0,057	2,870	0,023	0,815	-0,532	0,814	0,512	0,3966	-0,684	0,9556
Toff²	2,091	-0,436	2,280	1,161	2,100	-0,277	1,459	0,553	0,5941	-0,589	0,4094
C²	1,415	4,706	4,380	3,093	4,393	12,800	0,673	0,34	0,1332	-0,957	4,1001
I*Ton	0,279	-1,593	-1,090	0,627	1,191	-1,322	-0,519	-0,24	-0,9934	-0,662	-1,3543
I*Toff	-5,253	1,193	3,360	0,879	1,275	-0,824	1,412	-0,224	1,0011	-0,591	-3,0395
I*C	-1,796	-0,105	3,490	-0,232	-0,498	-2,368	0,399	0,462	-1,5297	-0,618	-1,8014
Ton*To:	0,326	2,071	4,170	0,681	0,618	1,420	-1,304	-0,418	-1,9238	0,061	1,0639
Ton*C	-1,399	1,322	1,930	1,072	1,107	2,264	0,789	0,431	0,7349	-3,468	1,0226
Toff*C	3,795	3,683	2,800	-1,196	0,708	1,092	0,67	0,702	-0,4978	2,299	-0,7907

Table 4.10 Mathematical Models of Ti64-Copper MRR

TiCu	3mm	2,5mm	2mm	1,5mm	1mm	0,9mm	0,8mm	0,7mm	0,6mm	0,5mm	0,4mm
MRR=	MRR=	MRR=	MRR=	MRR=	MRR=	MRR=	MRR=	MRR=	MRR=	MRR=	MRR=
Constan	62,060	44,647	906,105	310,519	83,217	252,216	-84,0872	-106,169	-118,644	-100,867	-170,377
I	5,387	6,449	-120,387	-26,585	-4,448	-8,514	-10,1545	13,878	9,152	15,438	7,316
Ton	3,556	3,989	-39,858	6,571	-5,463	-19,446	30,9619	0,471	-3,328	0,733	7,999
Toff	-4,245	-1,924	-20,344	-5,460	-8,807	-0,336	15,1872	14,147	24,479	21,183	13,641
C	6,818	9,984	-81,251	-67,467	-0,034	-39,833	-4,7885	7,572	6,972	-5,8	23,465
I²	3,377	6,837	5,445	1,906	0,609	-1,518	1,0142	-1,245	-0,554	0,307	-0,165
Ton²	0,665	1,888	-0,351	1,388	0,256	-1,361	-1,0339	-0,03	-0,056	-0,138	-0,493
Toff²	1,318	2,275	0,995	2,152	0,571	-0,615	-1,4135	-0,641	-0,209	0,027	-0,805
C²	2,057	1,877	2,829	2,661	-0,671	-0,988	-0,4887	-0,79	-1,044	-0,216	-0,632
I*Ton	-2,805	0,435	3,838	-0,894	-0,587	3,053	-1,1242	-0,447	0,635	-0,823	-0,036
I*Toff	0,836	0,164	-0,951	-0,612	0,031	3,905	0,5349	1,19	-1,073	-1,963	-0,485
I*C	0,147	0,658	4,618	2,150	0,053	-2,294	0,0739	-0,329	0,297	-0,054	-0,227
Ton*To:	2,678	2,488	0,855	-4,275	0,004	-5,472	-1,1374	-0,956	-1,282	-0,618	0,894
Ton*C	0,080	0,813	1,865	1,799	0,992	7,896	-0,0956	1,421	1,327	1,801	-1,175
Toff*C	2,159	-2,840	0,469	1,173	-0,031	2,373	1,1845	-0,958	-0,786	-0,586	-0,76

Table 4.11 Mathematical Models of IN718-Brass EWR

NiBr	3mm	2,5mm	2mm	1,5mm	1mm	0,9mm	0,8mm	0,7mm	0,6mm	0,5mm	0,4mm
EWR=	EWR=	EWR=	EWR=	EWR=	EWR=	EWR=	EWR=	EWR=	EWR=	EWR=	EWR=
Constan	0,382	0,703	13,500	26,250	65,714	139,163	143,741	173,030	-3,053	-507,321	-469,824
I	0,141	0,113	-2,101	-3,397	-6,769	-22,022	-13,226	-28,365	-5,982	104,309	28,912
Ton	0,111	0,080	-0,313	-1,036	-1,441	-4,673	-7,158	-8,722	10,441	90,232	105,168
Toff	-0,042	0,014	-0,117	-0,917	-1,418	-1,622	-5,088	-0,089	3,009	60,939	-25,770
C	0,078	0,220	-1,767	-2,876	-11,034	-15,333	-19,140	-16,462	-7,748	-112,304	46,632
I²	0,066	-0,013	0,165	0,297	0,245	1,203	0,777	1,358	0,932	-6,515	-1,798
Ton²	0,045	-0,009	0,038	0,099	0,239	0,275	0,425	0,593	0,908	-4,057	-3,067
Toff²	-0,002	-0,001	0,070	0,109	0,280	0,350	0,396	0,541	1,442	-4,043	-1,679
C²	0,040	0,022	0,118	0,256	0,709	1,153	1,187	1,394	1,297	10,741	-2,249
I*Ton	0,030	0,021	-0,029	-0,082	-0,205	0,103	-0,042	0,375	0,215	-0,431	-3,130
I*Toff	-0,020	-0,049	-0,038	-0,013	0,211	0,275	-0,024	0,125	-1,366	1,017	2,730
I*C	0,033	0,059	0,068	0,030	0,523	0,513	0,514	1,033	0,559	-1,858	-0,430
Ton*To:	-0,059	-0,024	-0,036	0,000	-0,273	-0,266	-0,037	-0,320	-2,047	-1,457	1,014
Ton*C	0,051	-0,008	0,047	0,047	0,228	0,322	0,308	0,038	-1,377	-2,514	-5,938
Toff*C	-0,060	-0,027	-0,049	-0,081	-0,324	-0,510	-0,034	-0,989	-0,392	-0,298	2,828

Table 4.12 Mathematical Models of IN718-Copper EWR

NiCu	3mm	2,5mm	2mm	1,5mm	1mm	0,9mm	0,8mm	0,7mm	0,6mm	0,5mm	0,4mm
EWR=	EWR=	EWR=	EWR=	EWR=	EWR=	EWR=	EWR=	EWR=	EWR=	EWR=	EWR=
Constan	0,429	0,523	7,634	6,614	42,043	93,834	92,947	103,808	65,104	167,998	320,955
I	0,090	0,091	-0,694	-1,297	-6,084	-13,200	-6,612	-5,073	-1,879	-10,190	-19,536
Ton	0,016	0,005	-0,301	0,315	-3,842	-1,521	-1,729	-1,834	6,402	-17,761	-17,412
Toff	-0,004	0,026	0,207	0,077	0,279	-0,561	-1,921	-1,841	-14,105	-7,073	-8,928
C	0,117	0,180	-1,714	-1,244	-3,505	-13,847	-18,490	-23,424	-11,316	-17,846	-48,599
I²	-0,012	0,003	0,029	0,095	0,435	0,546	0,301	0,070	0,164	1,417	-0,074
Ton²	-0,004	0,000	0,030	0,044	0,125	0,014	0,069	-0,018	0,221	1,173	1,122
Toff²	-0,011	-0,017	0,002	0,034	0,139	-0,011	0,020	0,001	0,238	1,021	0,189
C²	0,037	0,050	0,047	0,160	0,251	0,541	0,743	0,735	0,166	2,180	1,748
I*Ton	0,034	0,019	-0,003	-0,005	0,075	0,036	-0,265	-0,236	-0,915	0,044	0,963
I*Toff	-0,017	-0,060	-0,023	-0,002	0,017	0,314	0,001	0,058	0,324	-1,387	0,126
I*C	0,024	-0,041	0,088	0,031	-0,060	0,551	0,712	0,867	0,637	0,212	2,119
Ton*To:	-0,001	0,018	-0,057	-0,038	-0,132	-0,270	-0,007	-0,192	0,030	0,974	-0,584
Ton*C	-0,041	0,019	0,048	-0,082	0,403	0,482	0,407	0,789	-0,478	-0,719	0,312
Toff*C	-0,038	0,064	0,051	-0,049	-0,224	0,066	0,250	0,430	1,297	-0,730	1,193

Table 4.13 Mathematical Models of Ti64-Brass EWR

TiBr	3mm	2,5mm	2mm	1,5mm	1mm	0,9mm	0,8mm	0,7mm	0,6mm	0,5mm	0,4mm
EWR=	EWR=	EWR=	EWR=	EWR=	EWR=	EWR=	EWR=	EWR=	EWR=	EWR=	EWR=
Constan	0,260	0,205	13,904	6,312	26,508	18,280	13,974	12,686	-5,272	136,442	-444,512
I	0,071	0,088	-0,967	-1,220	-1,877	1,421	-1,071	-0,304	1,691	-1,038	56,871
Ton	0,010	0,029	-0,661	-0,151	-1,881	-1,984	-0,209	-0,367	1,028	4,405	19,637
Toff	-0,003	0,018	-1,065	0,028	-1,628	-1,573	-1,567	-1,159	-1,342	-30,227	-9,018
C	0,077	0,129	-1,445	-0,667	-2,644	-3,526	-1,251	-1,736	0,426	-0,620	78,412
I^2	0,032	0,073	0,035	0,087	0,067	0,065	0,040	0,004	0,105	-0,879	-2,606
Ton^2	0,003	0,000	0,025	-0,003	0,058	0,058	0,047	0,049	0,211	0,254	-0,943
$Toff^2$	-0,002	0,007	0,040	0,014	0,077	0,060	0,069	0,046	0,200	2,142	0,426
C^2	0,009	0,044	0,055	0,087	0,210	0,222	0,042	0,027	0,067	-0,202	-3,642
I*Ton	-0,012	-0,033	-0,012	0,010	0,066	-0,096	-0,032	-0,039	-0,241	3,581	1,446
I*Toff	-0,055	0,031	0,029	-0,006	0,086	-0,095	0,102	0,007	0,278	-2,260	1,117
I*C	-0,013	0,044	0,060	0,011	-0,014	-0,149	0,016	0,072	-0,476	0,571	-4,899
Ton*To:	0,006	-0,013	0,024	0,025	0,023	0,116	-0,063	-0,027	-0,527	-0,631	-1,001
Ton*C	-0,010	0,024	0,040	-0,003	0,071	0,169	0,042	0,028	0,267	-3,764	-0,906
Toff*C	-0,020	0,057	0,017	-0,056	-0,034	0,091	0,045	0,090	-0,021	2,539	-0,031

Table 4.14 Mathematical Models of Ti64-Copper EWR

TiCu	3mm	2,5mm	2mm	1,5mm	1mm	0,9mm	0,8mm	0,7mm	0,6mm	0,5mm	0,4mm
EWR=	EWR=	EWR=	EWR=	EWR=	EWR=	EWR=	EWR=	EWR=	EWR=	EWR=	EWR=
Constan	0,111	0,071	2,761	4,317	-0,158	4,385	1,381	-3,025	-8,646	-31,916	-69,342
I	0,036	0,031	-0,408	-0,395	-0,152	-0,153	-1,028	0,347	0,795	2,793	5,168
Ton	0,007	0,004	-0,293	-0,006	-0,043	-0,307	0,748	-0,076	0,160	0,911	3,143
Toff	0,002	-0,004	0,088	-0,070	-0,111	0,256	0,305	0,038	0,920	3,786	1,140
C	0,049	0,051	-0,224	-0,908	0,344	-1,130	-0,424	0,602	0,700	1,703	12,126
I^2	0,006	0,026	0,025	0,025	0,023	0,009	0,080	-0,025	-0,046	0,105	0,176
Ton^2	-0,003	0,012	0,009	0,017	0,009	-0,011	-0,029	0,003	-0,009	0,036	0,058
$Toff^2$	0,002	0,008	0,008	0,023	0,006	0,027	-0,028	-0,005	-0,023	-0,017	0,112
C^2	0,028	0,015	0,030	0,043	-0,005	0,031	0,018	-0,010	-0,040	0,084	-0,331
I*Ton	-0,007	-0,001	0,018	-0,023	-0,009	0,002	-0,019	0,004	0,028	0,016	0,326
I*Toff	0,008	-0,010	-0,026	-0,012	0,005	-0,007	0,018	0,042	-0,045	-0,441	-0,470
I*C	0,018	0,008	0,023	0,051	-0,016	0,011	-0,003	-0,044	0,001	-0,136	-0,815
Ton*To:	0,007	0,015	0,020	-0,021	0,010	-0,056	-0,029	0,000	-0,016	0,032	-0,167
Ton*C	0,000	-0,013	-0,015	0,013	-0,011	0,127	0,001	0,006	-0,004	-0,207	-0,687
Toff*C	0,012	-0,019	-0,026	-0,004	-0,011	-0,028	0,024	-0,035	-0,029	-0,109	0,190

Table 4.15 Mathematical Models of IN718-Brass Ra

NiBr	3mm	2,5mm	2mm	1,5mm	1mm	0,9mm	0,8mm	0,7mm	0,6mm	0,5mm	0,4mm
Ra=	Ra=	Ra=	Ra=	Ra=	Ra=	Ra=	Ra=	Ra=	Ra=	Ra=	Ra=
Constan	92,304	26,859	-126,334	-126,165	-15,900	-201,668	-141,751	-177,778	-201,901	-137,040	54,791
I	4,895	1,034	19,012	18,457	-3,516	28,756	26,517	28,345	13,264	8,453	-11,302
Ton	-10,369	-0,743	3,319	4,887	5,120	5,595	5,449	-0,720	-0,793	17,903	-15,815
Toff	-7,485	-4,711	3,646	3,623	-1,910	9,673	3,982	10,297	22,186	-8,880	-0,294
C	-9,823	-1,557	17,009	15,930	11,014	22,197	14,076	23,703	28,713	29,715	13,095
I^2	-0,326	-0,125	-1,247	-1,193	-0,141	-1,457	-1,447	-2,031	-0,320	-0,120	0,354
Ton^2	0,690	0,055	-0,323	-0,191	0,005	0,029	-0,255	0,227	-0,049	-0,724	0,845
$Toff^2$	0,502	0,160	-0,235	-0,315	-0,127	-0,550	-0,364	-0,631	-1,109	0,678	-0,337
C^2	0,004	-0,059	-1,250	-1,278	-1,115	-1,656	-1,588	-1,771	-0,793	-1,422	0,053
I*Ton	0,243	0,020	-0,122	-0,237	0,043	-0,330	-0,739	-0,050	0,361	0,126	0,562
I*Toff	-0,095	0,038	0,006	0,042	0,521	-0,300	-0,089	-0,018	-0,411	0,085	0,708
I*C	-0,178	0,063	-0,189	-0,121	0,226	-0,629	-0,165	-0,019	-1,193	-1,127	-0,389
Ton*To:	-0,731	0,023	0,200	0,022	-0,352	-0,333	0,051	0,029	0,639	-0,137	0,936
Ton*C	0,600	-0,053	0,096	-0,083	-0,414	-0,140	0,436	-0,354	-0,702	-0,930	-0,890
Toff*C	0,758	0,270	-0,269	0,017	0,358	0,300	0,201	-0,233	-1,119	-0,075	-0,768

Table 4.16 Mathematical Models of IN718-Copper Ra

NiCu	3mm	2,5mm	2mm	1,5mm	1mm	0,9mm	0,8mm	0,7mm	0,6mm	0,5mm	0,4mm
Ra=	Ra=	Ra=	Ra=	Ra=	Ra=	Ra=	Ra=	Ra=	Ra=	Ra=	Ra=
Constan	140,699	38,623	-61,590	-104,046	-81,551	-91,693	6,958	163,313	-30,704	-73,098	-42,220
I	-13,333	-5,684	12,536	14,303	12,801	11,795	5,713	-8,796	6,926	-5,099	20,136
Ton	-10,371	-1,394	1,150	1,169	3,187	-3,087	1,933	-8,436	1,173	10,329	-0,991
Toff	-10,202	-1,297	0,991	5,796	3,930	18,839	-12,814	-23,735	10,110	22,952	6,463
C	-4,248	-0,447	9,036	15,079	10,238	3,726	9,212	-0,898	-5,758	-1,973	-11,291
I²	0,238	0,306	-0,840	-1,011	-0,845	-0,101	-0,730	-0,026	0,268	0,149	-0,497
Ton²	0,193	0,000	-0,103	-0,147	-0,234	0,940	-0,087	1,004	0,300	0,081	-0,349
Toff²	0,260	0,100	0,005	-0,345	-0,179	-0,530	0,436	0,805	0,342	-0,984	-0,758
C²	0,213	-0,020	-0,811	-1,199	-1,036	0,037	-0,898	0,183	0,233	-0,324	0,554
I*Ton	0,405	0,048	-0,010	0,076	-0,032	-0,549	-0,390	0,559	-0,225	0,182	-0,380
I*Toff	0,384	-0,123	-0,021	-0,043	-0,145	-0,878	0,525	0,372	-1,033	-0,123	-0,792
I*C	0,588	0,261	-0,118	-0,113	-0,040	-0,116	0,459	0,347	-0,254	0,239	-0,596
Ton*To:	0,945	0,244	-0,047	0,042	-0,112	-0,314	0,589	0,487	-1,007	-1,600	0,719
Ton*C	-0,225	-0,095	0,091	-0,002	0,143	-0,514	-0,248	-1,805	0,405	-0,065	0,458
Toff*C	-0,344	-0,158	-0,079	-0,113	0,049	-0,415	-0,190	0,841	-0,067	0,413	0,643

Table 4.17 Mathematical Models of Ti64-Brass Ra

TiBr	3mm	2,5mm	2mm	1,5mm	1mm	0,9mm	0,8mm	0,7mm	0,6mm	0,5mm	0,4mm
Ra=	Ra=	Ra=	Ra=	Ra=	Ra=	Ra=	Ra=	Ra=	Ra=	Ra=	Ra=
Constan	-42,143	-48,526	-147,121	-118,941	-53,529	-72,828	-27,152	135,558	-4,077	120,488	209,253
I	10,959	-5,468	13,954	15,644	9,040	13,495	5,904	-6,061	9,093	-0,780	-17,328
Ton	8,608	6,633	7,022	6,397	-4,107	7,373	6,496	-5,660	-5,149	-1,438	-9,186
Toff	-4,085	6,803	6,142	4,740	-0,681	-0,030	3,349	-8,329	3,211	-15,707	-21,394
C	3,020	7,502	21,183	14,651	19,101	7,214	-0,565	-11,240	-1,126	-10,997	-8,266
I²	-0,629	1,006	-0,737	-1,308	-1,042	-0,954	-0,654	-0,867	-0,257	-0,182	0,345
Ton²	-0,624	-0,027	-0,458	-0,568	-0,060	-0,256	-0,333	-0,328	0,190	-0,066	-0,274
Toff²	0,400	-0,095	-0,413	-0,148	-0,253	-0,158	-0,124	-0,438	-0,139	1,368	0,536
C²	-0,528	-0,215	-1,681	-1,197	-1,131	-0,883	-0,463	-1,130	-0,508	-0,507	-0,555
I*Ton	-0,295	0,791	-0,154	0,193	0,297	-0,379	-0,128	-0,327	-0,239	-0,251	-0,057
I*Toff	0,005	-0,860	-0,040	-0,041	0,494	0,009	0,237	0,366	-0,506	0,615	0,551
I*C	-0,078	-0,982	-0,322	0,133	-0,144	0,251	0,259	2,444	-0,111	0,039	1,275
Ton*To:	-0,044	-0,876	-0,067	-0,041	0,573	0,057	-0,435	1,152	-0,001	-1,551	1,289
Ton*C	0,417	-0,737	0,153	0,038	-0,244	-0,203	0,273	0,555	0,575	2,106	0,677
Toff*C	-0,196	0,876	0,066	-0,325	-0,501	0,196	-0,028	0,551	0,400	0,277	0,163

Table 4.18 Mathematical Models of Ti64-Copper Ra

TiCu	3mm	2,5mm	2mm	1,5mm	1mm	0,9mm	0,8mm	0,7mm	0,6mm	0,5mm	0,4mm
Ra=	Ra=	Ra=	Ra=	Ra=	Ra=	Ra=	Ra=	Ra=	Ra=	Ra=	Ra=
Constan	16,258	-19,424	-81,856	-61,234	-82,657	-64,790	-41,292	-55,764	-9,587	-27,334	1,671
I	-11,117	2,041	13,158	1,441	7,315	12,083	3,361	-1,186	0,139	10,100	12,069
Ton	11,958	-0,378	1,832	10,526	7,677	-0,510	-3,168	7,054	10,271	-8,127	-47,522
Toff	1,484	0,922	5,225	2,224	4,511	-2,751	-1,627	3,019	-9,200	0,803	23,287
C	-3,132	5,008	9,930	8,972	10,323	14,244	17,391	9,269	3,230	7,879	18,172
I²	0,381	0,083	-0,987	-0,495	-0,523	-0,946	-0,774	0,617	-0,017	-0,525	-0,730
Ton²	-0,163	0,128	-0,182	-0,756	-0,523	0,059	-0,115	-0,101	-0,283	0,151	2,734
Toff²	0,129	0,106	-0,281	-0,179	-0,561	0,124	-0,068	-0,111	0,077	-0,073	-1,603
C²	0,376	-0,077	-0,951	-1,310	-0,980	-1,100	-1,665	-0,382	0,051	-0,325	-1,456
I*Ton	-0,018	0,006	-0,132	0,116	0,637	0,026	0,454	-0,199	-0,227	0,152	0,173
I*Toff	0,462	-0,298	0,230	0,400	-0,653	0,066	0,448	-0,067	0,094	-0,546	-0,469
I*C	0,334	-0,186	-0,086	0,288	-0,040	0,045	0,212	-0,765	0,177	-0,004	0,020
Ton*To:	-0,608	0,149	-0,158	-0,591	0,101	0,113	-0,052	-0,446	0,603	0,979	0,442
Ton*C	-0,696	-0,327	0,357	0,490	-0,812	-0,159	0,376	-0,115	-1,308	-0,256	0,302
Toff*C	-0,291	-0,184	-0,227	0,200	1,025	-0,036	-0,008	0,245	0,555	-0,354	-0,092

4.3.2 ANOVA Test for the generated mathematical models

Analysis of variance (ANOVA) for the adequacy of the developed models was then performed in the next step. The usual method for testing the adequacy of a model is carried out by computing the F-ratio of the lack of fit to the pure error and comparing it with the standard value. These values of P (< α-level) in the analysis ascertain that the regression model is significant. Therefore, one of the terms in the regression equation makes a significant impact on the mean response. For instance, if the F ratio is calculated for %95 level of confidence, the value which are less then 0.05 are considered significant and the values greater than 0.05 are not significant and the model is adequate to represent the relationship between EDM hole drilling responses and the EDM hole drilling process parameters. R^2 and adjusted R^2 are the two criteria which test the lack of fit of the generated empirical model. Selection of the level of confidence and the acceptable R^2 and adjusted R^2 percentages depend on the nature of the process to be modelled and the number of factors (inputs) and responses. If the process to be modelled has multi-factors and multi-responses, then the modelling of this process would not be easy, since the fitting ability of the generated empirical models decreases.

In this work, ANOVA test was performed to all the mathematical models in order to find the significant and non-significant factors. An example test was performed to D2NiBr and the calculated F-values, P-values, R^2 and adjusted R^2 percentages are shown in Table 4.19, 4.20 and 4.21 for MRR, EWR and Ra responses. In the given tables, the input process variables are designated as C5: (I), C6: (Ton), C7: (Toff), C8: (C).

R^2 and adjusted R^2 percentages shows the fitting ability of the generated second order polynomials to the experimental results. In the example ANOVA test, acceptable percentages of R^2 and adjusted R^2 values were obtained. For the rest of the diameters, these values were calculated in the range of 70% to 90%.

Table 4.19 D2NiBr MRR ANOVA test

Term	Coef	SE Coef	T	P
Constant	471,989	388,065	1,216	0,242
C5	-50,105	42,551	-1,178	0,256
C6	-25,064	42,551	-0,589	0,564
C7	-13,223	42,551	-0,311	0,760
C8	-53,291	42,551	-1,252	0,228
C5*C5	6,615	1,984	3,334	0,004
C6*C6	2,650	1,984	1,335	0,200
C7*C7	2,118	1,984	1,067	0,302
C8*C8	3,889	1,984	1,960	0,068
C5*C6	-1,591	2,653	-0,600	0,557
C5*C7	-1,997	2,653	-0,753	0,462
C5*C8	-0,680	2,653	-0,256	0,801
C6*C7	-0,835	2,653	-0,315	0,757
C6*C8	1,952	2,653	0,736	0,472
C7*C8	0,163	2,653	0,062	0,952

S = 10,61 R-Sq = 85,5% R-Sq(adj) = 72,8%

Analysis of Variance for MRR

Source	DF	Seq SS	Adj SS	Adj MS	F	P
Regression	14	10618,6	10618,6	758,47	6,74	0,000
Linear	4	8783,8	275,1	68,78	0,61	0,661
Square	4	1650,6	1650,6	412,65	3,67	0,027
Interaction	6	184,2	184,2	30,71	0,27	0,942
Residual Error	16	1801,2	1801,2	112,57		
Lack-of-Fit	10	1630,8	1630,8	163,08	5,74	0,022
Pure Error	6	170,4	170,4	28,39		
Total	30	12419,8				

Table 4.20 D2NiBr EWR ANOVA test

Term	Coef	SE Coef	T	P
Constant	13,4995	8,75521	1,542	0,143
C5	-2,1008	0,96000	-2,188	0,044
C6	-0,3132	0,96000	-0,326	0,748
C7	-0,1172	0,96000	-0,122	0,904
C8	-1,7666	0,96000	-1,840	0,084
C5*C5	0,1654	0,04476	3,694	0,002
C6*C6	0,0379	0,04476	0,846	0,410
C7*C7	0,0696	0,04476	1,555	0,139
C8*C8	0,1176	0,04476	2,627	0,018
C5*C6	-0,0286	0,05984	-0,477	0,640
C5*C7	-0,0382	0,05984	-0,638	0,532
C5*C8	0,0682	0,05984	1,139	0,271
C6*C7	-0,0358	0,05984	-0,598	0,558
C6*C8	0,0466	0,05984	0,778	0,448
C7*C8	-0,0493	0,05984	-0,824	0,422

S = 0,2394 R-Sq = 85,7% R-Sq(adj) = 73,2%

Analysis of Variance for EWR

Source	DF	Seq SS	Adj SS	Adj MS	F	P
Regression	14	5,48756	5,48756	0,391968	6,84	0,000
Linear	4	4,15737	0,41455	0,103637	1,81	0,177
Square	4	1,12528	1,12528	0,281321	4,91	0,009
Interaction	6	0,20490	0,20490	0,034149	0,60	0,729
Residual Error	16	0,91682	0,91682	0,057302		
Lack-of-Fit	10	0,87809	0,87809	0,087809	13,60	0,002
Pure Error	6	0,03873	0,03873	0,006456		
Total	30	6,40438				

Table 4.21 D2NiBr Ra ANOVA test

Term	Coef	SE Coef	T	P
Constant	-126,334	71,6904	-1,762	0,097
C5	19,012	7,8608	2,419	0,028
C6	3,319	7,8608	0,422	0,678
C7	3,646	7,8608	0,464	0,649
C8	17,009	7,8608	2,164	0,046
C5*C5	-1,247	0,3665	-3,401	0,004
C6*C6	-0,323	0,3665	-0,881	0,392
C7*C7	-0,235	0,3665	-0,640	0,531
C8*C8	-1,250	0,3665	-3,409	0,004
C5*C6	-0,122	0,4900	-0,250	0,806
C5*C7	0,006	0,4900	0,013	0,990
C5*C8	-0,189	0,4900	-0,385	0,705
C6*C7	0,200	0,4900	0,408	0,688
C6*C8	0,096	0,4900	0,196	0,847
C7*C8	-0,269	0,4900	-0,549	0,591

S = 1,960 R-Sq = 83,5% R-Sq(adj) = 69,0%

Analysis of Variance for SR

Source	DF	Seq SS	Adj SS	Adj MS	F	P
Regression	14	310,250	310,250	22,1607	5,77	0,001
Linear	4	226,771	34,162	8,5406	2,22	0,112
Square	4	80,724	80,724	20,1810	5,25	0,007
Interaction	6	2,755	2,755	0,4592	0,12	0,992
Residual Error	16	61,472	61,472	3,8420		
Lack-of-Fit	10	55,011	55,011	5,5011	5,11	0,029
Pure Error	6	6,460	6,460	1,0767		
Total	30	371,721				

In order to check the adequacy of the mathematical models, the level of significance (confidence level) must be determined prior to analysis. If this level is determined 90%, the critical p-value is to be 0.1. So that the p-values which are grater then 0.1 are regarded as non-significant factors and eliminated from the mathematical equations. Any p-values less than 0.1 are considered as significant or most significant factors and thus these factors are left in the equation to predict the responses. The ANOVA test was applied to D2NiBr and the reduced response equations were obtained for MRR, EWR and Ra in Table 4.22.

Table 4.22 Reduced response equations for D2NiBr

MRR = -53,291 C + 6,61 I^2 + 2,650 Ton^2 + 3,889 C^2 (Confidence level: 80%)
EWR = 13,49 + 2,100 I - 1,766 C + 0,16 I^2 + 0,069 $Toff^2$ + 0,1176 C^2 (Confidence level: 85%)
Ra = -126,334 + 19,012 I + 17,009 C - 1,247 I^2 - 1,25 C^2 (Confidence Level: 90%)

The determination of the significant (confidence) level is of primary importance in order to obtain well-fitted mathematical models with less error. For single response models and controlled testing environments, this significant level is commonly chosen as 95%. However, if there are multi-input factors and the effects of some of the process parameters are not considered, the level of significance may be varied. In this work, four input variables were considered and some of the other variables, such as dielectric pressure, polarity, electrode rotation speed were not included in the models. Thus, the confidence level was varied in order to consider the effects of factors as much as possible. The reduced mathematical models were then generated for the rest of the diameters. The reduced equations were tested with the validation experiments (to be explained in the latest of the chapter). It was found that the errors between the validation experimental results and the predicted values obtained from the reduced mathematical equations were not in acceptable percentages. Thus, all the input factors and their interactions were considered in the equations. In fact, R^2 and adjusted R^2 percentages of the models have also implied that the proposed models are adequate to illustrate the pattern of MRR, EWR and Ra for all eleven diameters and two different materials and electrodes.

4.3.3 Predicted and experimental results

Tables 4.23, 4.24, 4.25 and 4.26 give the experimental and predicted results obtained from the generated mathematical models. Percentage errors between these two results are also given for MRR, EWR and Ra in the same tables.

Table 4.23 Experimental and predicted results; percentage errors of D2NiBr

Exp. No	Exp_MRR	Exp_EWR	Exp_Ra	Pre_MRR	Pre_EWR	Pre_Ra	%Error MRR	%Error EWR	%Error Ra
1	0,062	0,384	10,941	0,064	0,433	11,651	-3,23	-12,76	-6,49
2	0,093	0,866	12,054	0,095	1,019	10,547	-2,15	-17,67	12,50
3	0,128	1,825	3,982	0,125	1,731	4,342	2,34	5,15	-9,04
4	0,107	1,655	3,771	0,108	1,582	3,963	-0,93	4,41	-5,09
5	0,081	0,814	12,809	0,082	0,729	11,328	-1,23	10,44	11,56
6	0,08	0,722	11,608	0,082	0,729	11,328	-2,50	-0,97	2,41
7	0,079	0,702	12,305	0,082	0,729	11,328	-3,80	-3,85	7,94
8	0,104	1,341	3,858	0,12	1,875	0,291	-15,38	-39,82	92,46
9	0,136	2,118	3,863	0,135	1,989	4,625	0,74	6,09	-19,73
1	0,119	1,612	4,357	0,11	1,385	6,404	7,56	14,08	-46,98
11	0,069	0,701	11,483	0,065	0,668	11,618	5,80	4,71	-1,18
12	0,089	0,814	10,513	0,082	0,729	11,328	7,87	10,44	-7,75
13	0,118	1,498	4,037	0,108	1,279	6,095	8,47	14,62	-50,98
14	0,083	0,779	12,086	0,091	0,961	11,109	-9,64	-23,36	8,08
15	0,102	0,827	10,659	0,11	0,985	10,311	-7,84	-19,11	3,26
16	0,147	1,962	3,545	0,134	1,839	5,198	8,84	6,27	-46,63
17	0,089	0,742	10,63	0,082	0,653	11,335	7,87	11,99	-6,63
18	0,093	1,194	4,672	0,084	0,978	6,336	9,68	18,09	-35,62
19	0,081	0,941	10,69	0,086	0,995	10,23	-6,17	-5,74	4,30
20	0,103	0,93	11,728	0,11	1,065	10,068	-6,80	-14,52	14,15
21	0,094	0,822	12,277	0,098	0,879	11,116	-4,26	-6,93	9,46
22	0,088	0,736	10,462	0,082	0,729	11,328	6,82	0,95	-8,28
23	0,084	0,736	11,592	0,082	0,729	11,328	2,38	0,95	2,28
24	0,075	0,623	10,312	0,075	0,695	10,005	0,00	-11,56	2,98
25	0,082	0,675	11,633	0,08	0,745	12,102	2,44	-10,37	-4,03
26	0,096	0,87	11,871	0,099	0,924	11,104	-3,13	-6,21	6,46
27	0,094	1,219	3,81	0,085	1,016	5,227	9,57	16,65	-37,19
28	0,114	1,812	4,447	0,115	1,697	5,047	-0,88	6,35	-13,49
29	0,063	0,611	11,105	0,083	0,941	7,486	-31,75	-54,01	32,59
30	0,085	0,85	10,767	0,075	0,523	12,368	11,76	38,47	-14,87
31	0,074	0,576	10,005	0,082	0,729	11,328	-10,81	-26,56	-13,22

Table .24 Experimental and predicted results; percentage errors of D2NiCu

Exp. No	Exp_MRR	Exp_EWR	Exp_Ra	Pre_MRR	Pre_EWR	Pre_Ra	%Error MRR	%Error EWR	%Error Ra
1	0,048	0,205	11,425	0,048	0,297	11,097	0,00	-44,88	2,87
2	0,054	0,379	10,199	0,059	0,503	9,634	-9,26	-32,72	5,54
3	0,082	1,476	4,054	0,079	1,262	4,396	3,66	14,50	-8,44
4	0,067	1,204	4,018	0,069	1,211	4,445	-2,99	-0,58	-10,63
5	0,05	0,461	9,565	0,055	0,566	9,679	-10,00	-22,78	-1,19
6	0,053	0,495	10,211	0,055	0,566	9,679	-3,77	-14,34	5,21
7	0,052	0,507	9,733	0,055	0,566	9,679	-5,77	-11,64	0,55
8	0,065	0,963	4,118	0,073	1,275	0,316	-12,31	-32,40	92,33
9	0,08	1,374	4,139	0,076	1,248	4,624	5,00	9,17	-11,72
1	0,075	1,009	3,626	0,066	0,731	5,369	12,00	27,55	-48,07
11	0,038	0,317	11,549	0,04	0,426	11,458	-5,26	-34,38	0,79
12	0,052	0,634	10,48	0,055	0,566	9,679	-5,77	10,73	7,64
13	0,065	0,726	3,479	0,066	0,836	5,224	-1,54	-15,15	-50,16
14	0,048	0,354	12,869	0,055	0,51	11,14	-14,58	-44,07	13,44
15	0,059	0,45	11,756	0,065	0,559	10,639	-10,17	-24,22	9,50
16	0,083	1,035	3,88	0,074	0,982	5,787	10,84	5,12	-49,15
17	0,057	0,419	10,946	0,053	0,395	10,913	7,02	5,73	0,30
18	0,059	0,548	3,692	0,054	0,442	5,189	8,47	19,34	-40,55
19	0,054	0,631	9,608	0,054	0,647	9,766	0,00	-2,54	-1,64
20	0,061	0,566	9,663	0,068	0,761	9,15	-11,48	-34,45	5,31
21	0,063	0,599	12,214	0,06	0,471	10,862	4,76	21,37	11,07
22	0,06	0,59	8,999	0,055	0,566	9,679	8,33	4,07	-7,56
23	0,058	0,55	9,369	0,055	0,566	9,679	5,17	-2,91	-3,31
24	0,054	0,667	9,277	0,052	0,611	9,383	3,70	8,40	-1,14
25	0,053	0,492	11,712	0,045	0,296	11,084	15,09	39,84	5,36
26	0,056	0,281	11,831	0,059	0,37	10,727	-5,36	-31,67	9,33
27	0,066	1,006	4,104	0,056	0,775	5,234	15,15	22,96	-27,53
28	0,059	0,894	3,841	0,065	0,968	4,483	-10,17	-8,28	-16,71
29	0,036	0,189	9,164	0,05	0,382	6,85	-38,89	-102,1	25,25
30	0,05	0,41	9,16	0,047	0,237	12,555	6,00	42,20	-37,06
31	0,058	0,727	9,399	0,055	0,566	9,679	5,17	22,15	-2,98

Table 4.25 Experimental and predicted results; percentage errors of D2TiBr

Exp. No	Exp_MRR	Exp_EWR	Exp_Ra	Pre_MRR	Pre_EWR	Pre_Ra	%Error MRR	%Error EWR	%Error Ra
1	0,058	0,282	10,306	0,062	0,338	11,166	-6,90	-19,86	-8,34
2	0,062	0,438	12,043	0,06	0,459	10,183	3,23	-4,79	15,44
3	0,094	0,95	4,628	0,09	0,824	5,473	4,26	13,26	-18,26
4	0,077	0,666	3,724	0,071	0,624	5,354	7,79	6,31	-43,77
5	0,035	0,189	11,67	0,049	0,268	11,973	-40,00	-41,80	-2,60
6	0,044	0,218	12,056	0,049	0,268	11,973	-11,36	-22,94	0,69
7	0,05	0,303	11,476	0,049	0,268	11,973	2,00	11,55	-4,33
8	0,071	0,613	3,94	0,08	0,781	-0,895	-12,68	-27,41	122,72
9	0,068	0,712	3,699	0,07	0,715	5,419	-2,94	-0,42	-46,50
1	0,075	0,659	3,952	0,065	0,55	6,233	13,33	16,54	-57,72
11	0,047	0,157	11,254	0,04	0,171	11,385	14,89	-8,92	-1,16
12	0,046	0,201	11,363	0,049	0,268	11,973	-6,52	-33,33	-5,37
13	0,072	0,515	4,161	0,071	0,546	6,446	1,39	-6,02	-54,91
14	0,04	0,217	12,894	0,049	0,257	12,318	-22,50	-18,43	4,47
15	0,048	0,26	12,096	0,052	0,254	12,031	-8,33	2,31	0,54
16	0,071	0,547	9,959	0,066	0,534	9,086	7,04	2,38	8,77
17	0,059	0,273	11,337	0,061	0,331	11,557	-3,39	-21,25	-1,94
18	0,061	0,489	4,047	0,059	0,397	5,228	3,28	18,81	-29,18
19	0,05	0,369	12,152	0,057	0,401	10,457	-14,00	-8,67	13,95
20	0,065	0,431	12,691	0,069	0,464	10,395	-6,15	-7,66	18,09
21	0,062	0,324	12,692	0,058	0,31	12,257	6,45	4,32	3,43
22	0,056	0,317	12,35	0,049	0,268	11,973	12,50	15,46	3,05
23	0,055	0,323	13,978	0,049	0,268	11,973	10,91	17,03	14,34
24	0,051	0,251	11,143	0,052	0,271	9,884	-1,96	-7,97	11,30
25	0,06	0,338	11,316	0,056	0,259	11,508	6,67	23,37	-1,70
26	0,062	0,188	11,153	0,06	0,297	11,823	3,23	-57,98	-6,01
27	0,053	0,36	3,94	0,048	0,297	5,71	9,43	17,50	-44,92
28	0,064	0,6	3,518	0,068	0,61	5,031	-6,25	-1,67	-43,01
29	0,042	0,218	11,65	0,052	0,284	8,968	-23,81	-30,28	23,02
30	0,058	0,311	10,113	0,054	0,195	11,393	6,90	37,30	-12,66
31	0,059	0,328	10,917	0,049	0,268	11,973	16,95	18,29	-9,67

Table 4.26 Experimental and predicted results; percentage errors of D2TiCu

Exp. No	Exp_MRR	Exp_EWR	Exp_Ra	Pre_MRR	Pre_EWR	Pre_Ra	%Error MRR	%Error EWR	%Error Ra
1	0,053	0,129	11,502	0,041	0,074	11,939	22,64	42,64	-3,80
2	0,043	0,105	11,133	0,046	0,169	9,101	-6,98	-60,95	18,25
3	0,05	0,146	4,426	0,066	0,216	4,507	-32,00	-47,95	-1,83
4	0,06	0,214	4,337	0,051	0,189	4,898	15,00	11,68	-12,94
5	0,036	0,062	10,601	0,034	0,08	10,642	5,56	-29,03	-0,39
6	0,036	0,066	9,715	0,034	0,08	10,642	5,56	-21,21	-9,54
7	0,035	0,096	10,753	0,034	0,08	10,642	2,86	16,67	1,03
8	0,061	0,295	4,047	0,06	0,34	0,672	1,64	-15,25	83,40
9	0,086	0,455	3,221	0,073	0,339	4,4	15,12	25,49	-36,60
1	0,03	0,069	4,566	0,038	0,127	6,459	-26,67	-84,06	-41,46
11	0,029	0,041	12,518	0,033	0,08	12,668	-13,79	-95,12	-1,20
12	0,028	0,05	11,077	0,034	0,08	10,642	-21,43	-60,00	3,93
13	0,045	0,18	4,356	0,035	0,109	5,649	22,22	39,44	-29,68
14	0,033	0,068	13,775	0,031	0,024	12,4	6,06	64,71	9,98
15	0,046	0,099	10,305	0,047	0,13	9,569	-2,17	-31,31	7,14
16	0,079	0,235	3,828	0,073	0,257	5,53	7,59	-9,36	-44,46
17	0,03	0,062	10,517	0,03	0,01	11,285	0,00	83,87	-7,30
18	0,05	0,306	3,204	0,041	0,25	5,687	18,00	18,30	-77,50
19	0,03	0,054	9,753	0,031	0,053	9,938	-3,33	1,85	-1,90
20	0,034	0,083	10,461	0,035	0,097	9,389	-2,94	-16,87	10,25
21	0,041	0,13	10,717	0,043	0,123	10,753	-4,88	5,38	-0,34
22	0,034	0,099	10,49	0,034	0,08	10,642	0,00	19,19	-1,45
23	0,034	0,102	10,453	0,034	0,08	10,642	0,00	21,57	-1,81
24	0,027	0,085	11,21	0,031	0,134	10,435	-14,81	-57,65	6,91
25	0,033	0,087	10,713	0,025	0,096	11,38	24,24	-10,34	-6,23
26	0,039	0,132	11,737	0,039	0,111	10,583	0,00	15,91	9,83
27	0,031	0,17	4,256	0,035	0,153	5,51	-12,90	10,00	-29,46
28	0,049	0,386	4,306	0,061	0,391	4,157	-24,49	-1,30	3,46
29	0,029	0,06	11,407	0,039	0,101	7,858	-34,48	-68,33	31,11
30	0,026	0,041	11,472	0,031	0,059	12,999	-19,23	-43,90	-13,31
31	0,035	0,083	11,403	0,034	0,08	10,642	2,86	3,61	6,67

4.4 Main effects and Interaction plots

A main effect is an outcome that is a consistent difference between levels of a factor. The main effects plots simply show the average outcome for each value or each variable, combining the effects of the other variables is if all variables were different. On the other hand, interaction plots illustrate the effects between variables which are not independent [23].

In this work, the main effects and interaction plots were produced for the input variables (I, Ton, Toff and C) and responses (MRR, EWR and Ra). D2NiBr was again chosen as a sample case and the same methodology used to obtain these plots was implemented to the rest of the diameters. The input variables are plotted as their machine settings and the MRR, EWR and Ra are plotted as mgr/min, mm/min and μm, respectively. The main effects graphs and interaction plots for D2 hole are all given in Appendices A and B.

4.4.1 Effects of EDM input parameters on MRR for D2NiBr

The relationship between the MRR and I, Ton, Toff, C is shown in Figure 4.1. It is evident from the main effect plot that the discharge current is the most prominent factor which affects MRR than the other variables. So that, when the discharge current is increased, the MRR also increases. Although increasing the pulse on time and the capacitance, the MRR increases. Pulse off time is not significant on MRR. Thus, each process variable is considered individually in the plots.

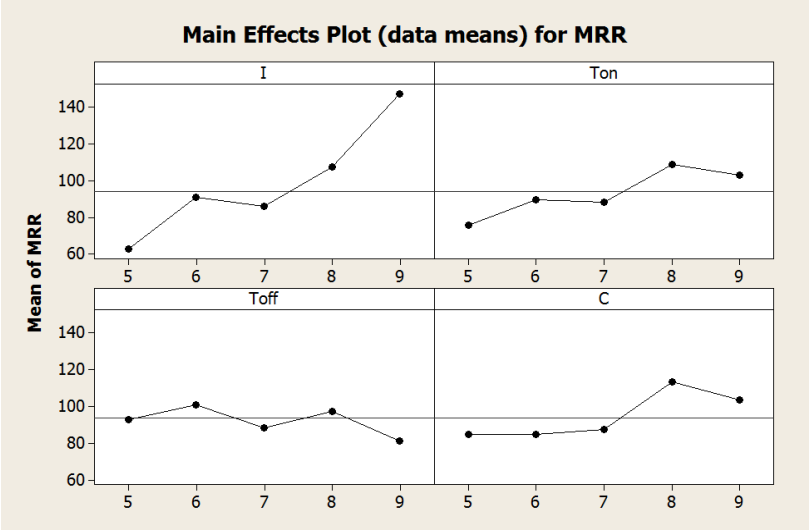

Figure 4.1 Main effects plot of D2NiBr for MRR

In the interaction plots, the input variables are considered together and their effects are analysed for MRR. Figure 4.2 shows the interaction plot of D2NiBr. When I and Ton considered together, their dual effect on MRR is shown by curves at their different settings. For instance, the interaction of I and Ton on MRR is increasing when both I and Ton settings are increased. Nevertheless the interaction of I-Toff and Ton-Toff on MRR show similar phenomenon. MRR decreases on the both

interactions. For the I-Toff interaction, decreasing the discharge current and increasing the pulse off time affect the MRR in a negative manner. Ton-Toff exhibits the similar case.

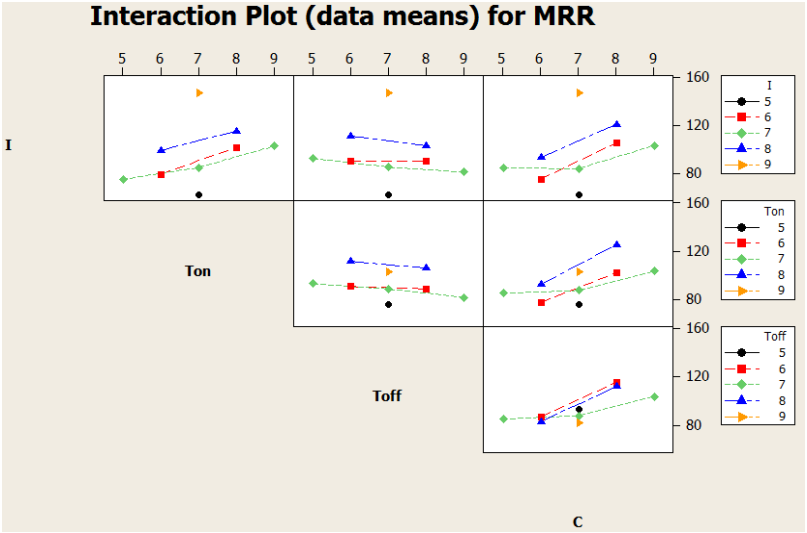

Figure 4.2 Interaction Plot of D2NiBr for MRR

4.4.2 Effects of EDM input parameters on EWR for D2NiBr

The main effects and interaction plots for EWR are shown in Figure 4.3 and 4.4, respectively. Discharge current has a substantial effect on EWR compared to the other input variables. Pulse on time and capacitance also affect the EWR. On the other hand, pulse off time has a limited effect on EWR. If the interaction plot is analysed, it can be said that the any input variable interact with capacitance has a prominent effect on ERW. So that, increasing of both interacted variables results with higher EWR. However, same situation is not valid for other interactions (I-Ton, I-Toff and Ton-Toff). For instance, I-Ton interaction, discharge current is primary factor that affects EWR, but Ton has limited effect. For I-Toff interaction, discharge current is the only factor that affects the EWR. Similarly, Ton is the primary factor affects the EWR for Ton-Toff interaction.

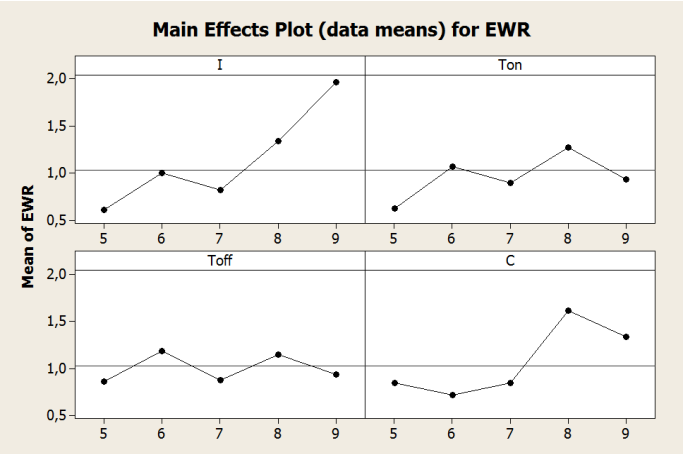

Figure 4.3 Main effects plot of D2NiBr for EWR

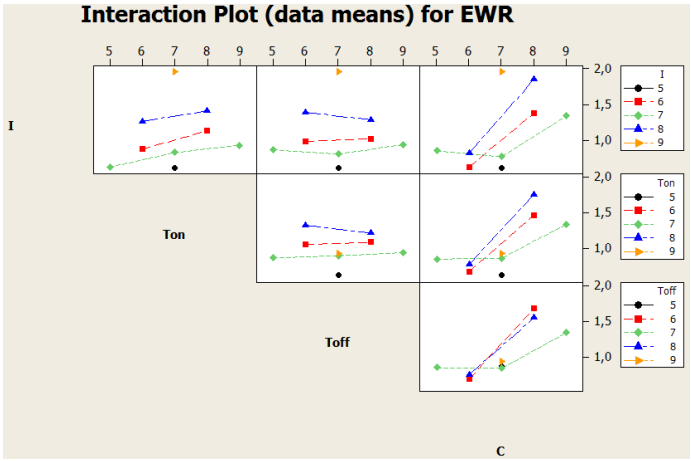

Figure 4.4 Interaction Plot of D2NiBr for EWR

4.4.3 Effects of EDM input parameters on Ra for D2NiBr

The main effects and interaction plots for Ra (surface roughness) are shown in Figure 4.5 and 4.6, respectively. It is very clear that all input variables individually affect on Ra. Particularly, increase in discharge current and capacitance of the EDM process produce very rough surfaces. However, increasing Ton and Toff influence the surface quality but it is limited in a range. Low capacitance settings have very adverse effects on surface roughness when it is interacted with the other variables. It is also evident that higher values of interacted variables produce smooth surface. I-Ton, I-Toff and Ton-Toff show almost similar attitudes. For I-Ton and I-Toff interactions, smooth surfaces are obtained at higher discharge current and moderate Ton and Toff rates. For Ton-Toff interaction, fairly rough surface is obtained at higher Ton settings and again moderate Toff rates.

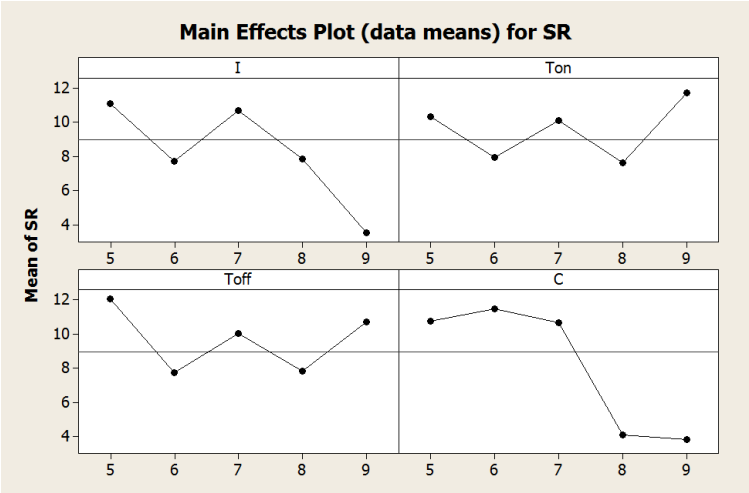

Figure 4.5 Main effects plot of D2NiBr for Ra

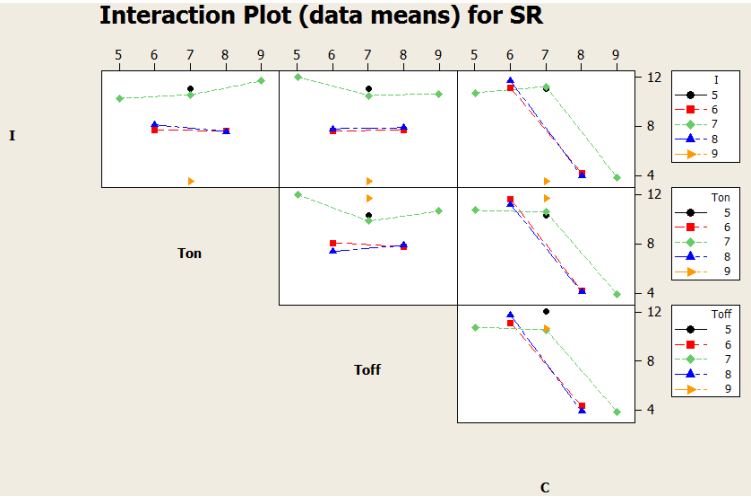

Figure 4.6 Interaction Plot of D2NiBr for Ra

4.5 Optimization of EDM fast hole drilling process

Process optimization is the discipline of adjusting a process so as to optimize some specified set of parameters without violating some constraint. The most common goals are minimizing cost, maximizing throughput, and/or efficiency. This is one of the major quantitative tools in industrial decision making [23].

Optimization of input parameter (factors) can easily automatic conducted with RSM and Minitab®. Use of response optimization is to help identify the combination of input variable settings that jointly optimize a single response or a set of responses. Joint optimization must satisfy the requirements for all the responses in the set, which is measured by the composite desirability.

Composite desirability (D) in response optimization is a measure of how the solution has satisfied the combined goals for all the responses. Composite desirability has a range of zero to one [0 to 1]. One (1) represents the ideal case; zero (0) indicates that one or more responses are outside their acceptable limits. Composite desirability is the weighted geometric mean of the individual desirability's for the responses. The algorithms generated in Minitab® calculate an optimal solution and draws a plot. The optimal solution serves as the starting point for the plot. This optimization plot allows you to interactively change the input variable settings to perform sensitivity analyses and possibly improve the initial solution. Once an optimization plot is created, the input variable settings can be changed. For factorial and response surface designs, the factor levels can be adjusted. For mixture designs, component, process variable, and amount variable settings can be adjusted. These input variable settings on the optimization plot might want to change for many reasons:

- To search for input variable settings with a higher composite desirability
- To search for lower-cost input variable settings with near optimal properties
- To explore the sensitivity of response variables to changes in the design variables
- To "calculate" the predicted responses for an input variable setting of interest
- To explore input variable settings in the neighbourhood of a local solution

When an input variable is changed to a new level, the graphs are redrawn and the predicted responses and desirability's are recalculated.

The main objective of this research is to model EDM hole drilling process for optimum operation representing a particular problem in the manufacturing environment where, it is not possible to define the optimization objective function using a smooth and continuous mathematical formula. It has been hard to establish models that accurately correlate the process variables and performance of EDM hole drilling process. Thus, an attempt was fulfilled to estimate the optimum drilling settings to build the best possible MRR, EWR and Ra within the predicted constraints. In the optimisation attempts, Ra was chosen the most important output factor than the other outputs. MRR and EWR are the second and third important factors in optimisations, respectively. All optimization functions were developed in this arrangement. Minitab® software and the response surface optimization tool

(response optimizer) were used for optimizing these outputs output. Firstly, optimization parameters were designated. Ra, MRR and EWR were optimized after their importance values were determined. Ra was the first important parameter and its importance was determined as 10. The next important parameter was MRR and its importance was determined as 6. Finally the least important parameter was EWR and its importance was determined as 3. The objective function of Ra and EWR optimisation was the minimisation of surface roughness and electrode wear rate. The objective function of MRR optimisation was the maximization of material removal rate. Ra and EWR target values were chosen their predicted minimum results. Ra and EWR upper limits were chosen their predicted maximum results. MRR target value was chosen its predicted maximum result and MRR minimum limit value was chosen its predicted minimum results in the RSM optimisation tool of Minitab. After necessary settings and the determination of constraints, the RSM optimisation were implemented in order to find the best possible EDM hole drilling settings for all the diameters and the materials. The optimum results found in the optimisation were then used to calculate optimum MRR, EWR and Ra using generated empirical equations. In order to evaluate the optimum input parameters in real case applications and obtain their output results, the confirmation experiments were conducted using the optimum input factors. An example of optimisation graphs and optimum results for ∅2 mm diameter drilled holes is discussed in the following section.

4.5.1 Optimization results of MRR, EWR and Ra for D2NiBr

Figure 4.7 shows the optimisation plots of D2NiBr for MRR, EWR and Ra (SR) and optimum results. These results also summarized as below.

C5 [I] =8.79≈9.00, C6 [Ton] =8.95≈9.00,

C7 [Toff] =5.08≈5.00, C8 [C] =5.00≈5.00 (EDM machine settings)

Combined or composite desirability of the three responses is D=0.99

Predict responses obtained from mathematical equations are;

Ra=3.48µm MRR=158.35 mgr/min EWR=1.599 mm/min

Experimental responses obtained from the conducted optimisation experiments are;

Ra=3.53µm MRR=254 mgr/min EWR=2.408 mm/min

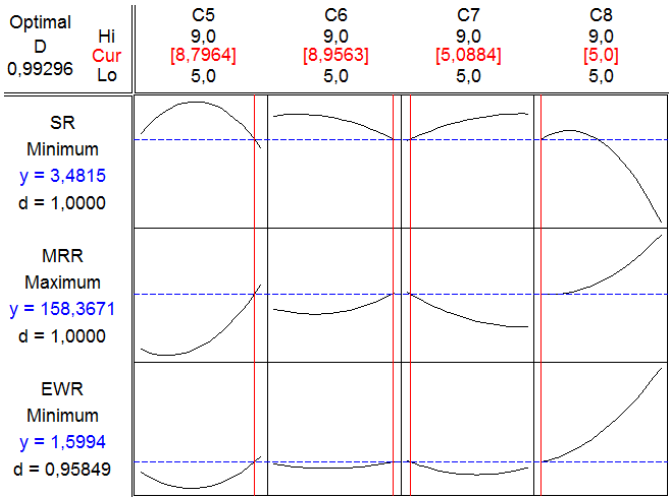

Figure 4.7 Optimization graphs and results of D2NiBr for MRR, EWR and Ra

4.5.2 Optimization of MRR, EWR and Ra for D2NiCu

Figure 4.8 shows the optimisation plots of D2NiCu for MRR, EWR and Ra (SR) and optimum results. These results also summarized as below.

C5 [I] =5.00≈5.00, C6 [Ton] =7.362≈7.00,

C7 [Toff] =5.00≈5.00, C8 [C] =9.00≈9.00 (EDM machine settings)

Combined or composite desirability of the three responses is D=0.86

Predict responses obtained from mathematical equations are;

Ra=1.78 µm MRR=69.64 mgr/min EWR=0.47 mm/min

Experimental responses obtained from the conducted optimisation experiments are;

Ra=3.50 µm MRR=72.00 mgr/min EWR=0.913 mm/min

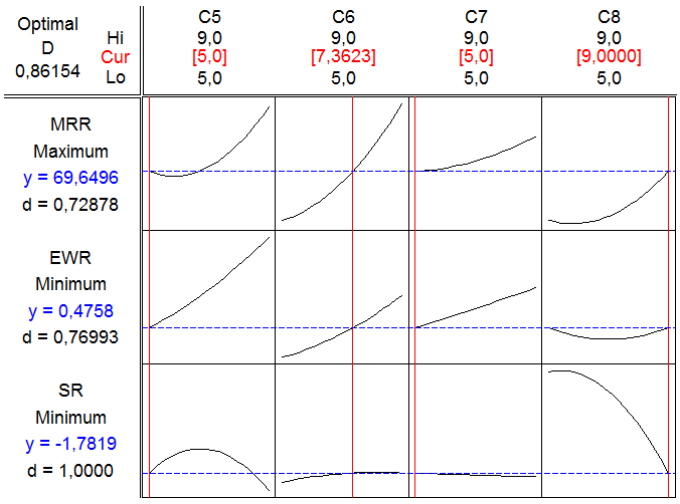

Figure 4.8 Optimization graphs and results of D2NiCu for MRR, EWR and Ra

4.5.3 Optimization of MRR, EWR and Ra for D2TiBr

Figure 4.9 shows the optimisation plots of D2TiBr for MRR, EWR and Ra (SR) and optimum results. These results also summarized as below.

C5 [I] =9.00≈9.00, C6 [Ton] =9.00≈9.00,

C7 [Toff] =9.00≈9.00, C8 [C] =5.00≈5.00 (EDM machine settings)

Combined or composite desirability of the three responses is D=0.84

Predict responses obtained from mathematical equations are;

Ra=4.77 µm MRR=92.08 mgr/min EWR=0.48 mm/min

Experimental responses obtained from the conducted optimisation experiments are;

Ra=3.77 µm MRR=121.00 mgr/min EWR=1.443 mm/min

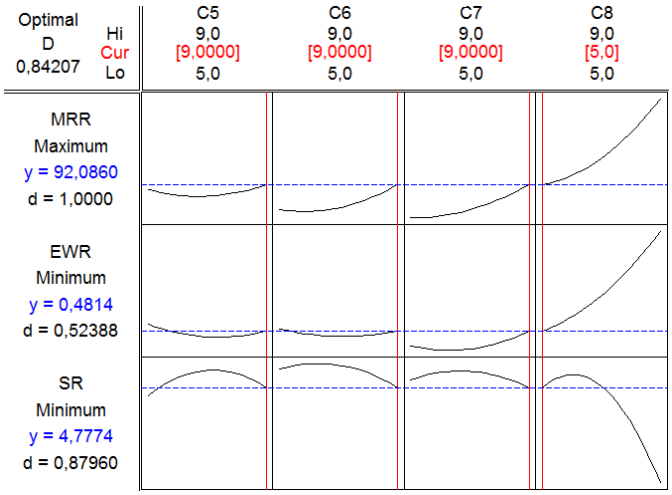

Figure 4.9 Optimization graphs and results of D2TiBr for MRR, EWR and Ra

4.5.4 Optimization of MRR, EWR and Ra for D2TiCu

Figure 4.10 shows the optimisation plots of D2TiCu for MRR, EWR and Ra (SR) and optimum results. These results also summarized as below.

C5 [I] =9.00≈9.00, C6 [Ton] =6.49≈6.00,

C7 [Toff] =8.99≈9.00, C8 [C] =7.64≈8.00 (EDM machine settings)

Combined or composite desirability of the three responses is D=0.91

Predict responses obtained from mathematical equations are;

Ra=3.21 µm MRR=71.52 mgr/min EWR=0.152 mm/min

Experimental responses obtained from the conducted optimisation experiments are;

Ra=3.70 µm MRR=56.00 mgr/min EWR=3.705 mm/min

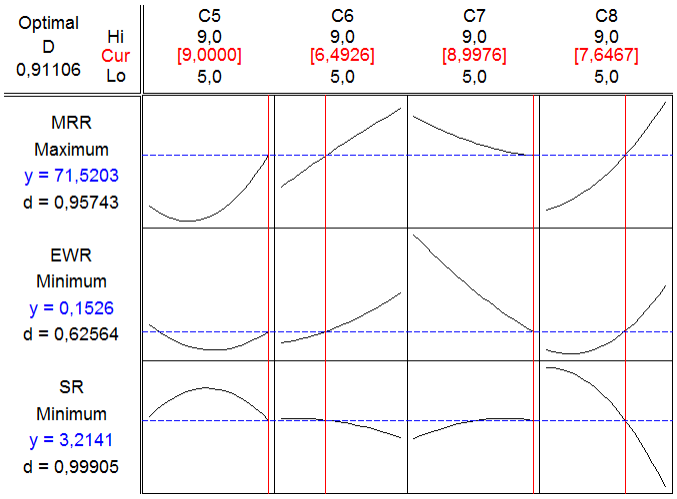

Figure 4.10 Optimization graphs and results of D2TiCu for MRR, EWR and Ra

There are some differences between predicted optimum results and optimum experimental results. These differences come from random errors (heat up of the machine, impurities of dielectric water, electrode and work-pieces chemical and physical constructions) and optimum input parameters round up and round down to machine setting and so on. Especially Ra provides some evidence about experiment and system. In this study, the most important aim was to obtain smooth surface, and thus the optimization was made in this direction. For some of the experiments especially under 0.8 mm diameter, fairly rough surfaces were unfortunately obtained. During the optimisation procedure was followed, Ra importance values were always entered at the highest but the system optimized the three output values together. Under 0,8 mm diameters, other outputs (MRR and EWR) were found dramatically decreasing and increasing, so that the RSM optimiser tried to make the balancing with Ra with the others. This situation also might affect the optimization results and cause rough surfaces. Table 4.27 shows the optimum experimental results.

Table 4.27 Optimization experiments results of EDM hole drilling

Ø (mm)	Materials	MRR mgr/min	EWR mm/min	Ra µm	Drilling rate min/mm	I	Ton	Toff	C	I(A)	Ton (µs)	Toff (µs)	C (µF)
3	NiBr	0,239	0,738	3,506	0,244	9	9	9	5	12	44	26	1100
	NiCu	0,098	0,523	3,698	0,606	8	9	6	7	11,5	44	18	1316
	TiBr	0,180	0,850	3,835	0,182	9	9	9	9	12	44	26	1476
	TiCu	0,067	0,170	3,125	0,485	5	9	9	8	8,2	44	26	1422
2,5	NiBr	0,121	1,157	2,392	0,303	9	6	8	8	12	30	23	1422
	NiCu	0,027	0,138	2,928	1,515	6	9	5	9	8,8	44	16	1476
	TiBr	0,089	0,501	3,101	0,221	5	5	5	9	8,2	27	16	1476
	TiCu	0,043	0,092	5,239	0,606	5	5	5	5	8,2	27	16	1100
2	NiBr	0,254	2,408	3,534	0,108	9	9	5	5	12	44	16	1100
	NiCu	0,072	0,913	3,500	0,398	5	7	5	9	8,2	35	16	1476
	TiBr	0,121	1,443	3,774	0,112	9	9	9	5	12	44	26	1100
	TiCu	0,056	0,282	3,705	0,248	9	7	9	8	12	35	26	1422
1,5	NiBr	0,082	1,610	3,010	0,182	5	5	9	8	8,2	27	26	1422
	NiCu	0,091	2,841	3,036	0,183	9	9	9	8	12	44	26	1422
	TiBr	0,069	1,626	3,254	0,094	9	5	5	5	12	27	16	1100
	TiCu	0,032	0,305	2,892	0,262	5	5	9	9	8,2	27	26	1476
1	NiBr	0,092	3,667	3,270	0,082	5	9	9	8	8,2	44	26	1422
	NiCu	0,045	2,562	3,288	0,152	6	6	9	9	8,8	30	26	1476
	TiBr	0,079	1,937	5,206	0,047	9	9	5	5	12	44	16	1100
	TiCu	0,011	0,050	4,818	0,523	5	5	9	5	8,2	27	26	1100
0,9	NiBr	0,079	5,617	4,201	0,071	5	6	8	9	8,2	30	23	1476
	NiCu	0,039	1,167	5,333	0,273	7	7	7	7	10,2	35	20	1316
	TiBr	0,043	2,773	5,639	0,068	9	5	9	8	12	27	26	1422
	TiCu	0,011	0,610	4,272	0,136	9	5	9	9	12	27	26	1476
0,8	NiBr	0,074	7,080	4,751	0,076	5	7	7	8	8,2	35	20	1422
	NiCu	0,065	5,470	3,780	0,085	5	9	5	9	8,2	44	16	1476
	TiBr	0,047	3,568	4,296	0,056	5	5	9	8	8,2	27	26	1422
	TiCu	0,037	0,564	6,746	0,152	5	9	8	5	8,2	44	23	1100
0,7	NiBr	0,086	16,000	7,253	0,045	7	9	9	8	10,2	44	26	1422
	NiCu	0,045	5,878	5,455	0,074	5	8	5	9	8,2	38	16	1476
	TiBr	0,018	1,885	4,993	0,102	5	5	9	9	8,2	27	26	1476
	TiCu	0,010	0,325	5,823	0,218	6	5	6	5	8,8	27	18	1100
0,6	NiBr	0,087	33,056	5,965	0,041	9	9	9	9	12	44	26	1476
	NiCu	0,025	2,080	8,922	0,227	8	9	9	6	11,5	44	26	1217
	TiBr	0,009	0,701	4,433	0,248	5	6	5	9	8,2	30	16	1476
	TiCu	0,007	0,187	7,232	0,430	5	5	7	5	8,2	27	20	1100
0,5	NiBr	0,096	40,380	5,913	0,033	5	9	9	9	8,2	44	26	1476
	NiCu	0,069	24,000	4,834	0,043	5	7	5	8	8,2	35	16	1422
	TiBr	0,026	3,729	5,468	0,047	5	6	8	9	8,2	30	23	1476
	TiCu	0,024	4,320	4,437	0,083	5	9	5	9	8,2	44	16	1476
0,4	NiBr	0,047	35,167	4,973	0,060	8	9	6	9	11,5	44	18	1476
	NiCu	0,026	15,100	5,052	0,100	5	5	5	9	8,2	27	16	1476
	TiBr	0,060	47,050	4,501	0,020	5	9	5	9	8,2	44	16	1476
	TiCu	0,027	33,733	6,217	0,030	9	6	5	9	12	30	16	1476

4.6 Validation Experiments

After generating the mathematical equations and producing the optimum results for MRR, EWR and Ra, the validation experiments were conducted in order to evaluate the effectiveness of the developed models. So that, five different validation experiments were designed via selecting the EDM machine settings which were not used in the conducted experiments. The designed experimental settings for validation are shown in Table 4.28. In total 220 validation experiments were conducted for 11 different materials, two different alloys and two electrode materials. The results obtained from the validation experiments were then compared with the results calculated from the mathematical models and shown in Table 4.29 for D2 experiments.

Table 4.28 Validation experiments input values

Experiment No	**Machine Setting**				**Real Values**			
	I	**Ton**	**Toff**	**C**	**I(A)**	**Ton(□ s)**	**Toff(□ s)**	**C(□ F)**
1	7	8	7	8	10,2	38	20	1422
2	8	7	7	6	11,5	35	20	1217
3	6	8	8	7	8,8	38	23	1316
4	6	7	8	9	8,8	35	23	1476
5	7	9	5	8	10,2	44	16	1422

Table 4.29 Comparisons of the validation results

Exp. #	D2	MRR(mg/min) Experimental	MRR(mg/min) Mathematical	MRR %Error	EWR(mm/min) Experimental	EWR(mm/min) Mathematical	EWR %Error	Ra(μm) Experimental	Ra(μm) Mathematical	Ra %Error
1	NiBr	152,68	110,53	27,60	1,82	1,36	25,08	3,29	6,764	-105,36
2	NiBr	134,00	94,74	29,30	1,25	0,83	33,21	10,74	11,387	-6,05
3	NiBr	117,94	90,10	23,61	0,88	0,90	-1,88	8,67	10,273	-18,46
4	NiBr	135,65	117,61	13,30	1,60	1,69	-5,10	5,09	0,951	81,32
5	NiBr	154,95	145,15	6,33	2,20	2,15	2,11	2,92	4,874	-67,09
1	NiCu	31,49	69,45	-120,52	0,35	0,99	-182,52	3,70	5,745	-55,08
2	NiCu	72,67	57,73	20,56	0,55	0,45	18,38	11,37	10,948	3,69
3	NiCu	76,00	54,12	28,79	0,71	0,52	27,29	8,87	8,973	-1,12
4	NiCu	61,63	73,20	-18,77	0,82	1,14	-39,62	3,95	0,11	97,22
5	NiCu	114,00	79,40	30,35	1,96	1,23	37,46	3,36	5,768	-71,73
1	TiBr	67,50	69,58	-3,08	0,60	0,58	3,42	3,70	7,065	-90,71
2	TiBr	80,00	50,40	37,00	0,67	0,21	68,17	11,33	12,989	-14,61
3	TiBr	60,30	59,16	1,89	0,27	0,35	-27,58	10,32	10,691	-3,59
4	TiBr	75,00	75,62	-0,83	0,59	0,67	-12,92	2,64	1,164	55,98
5	TiBr	79,50	72,53	8,77	0,67	0,81	-20,64	3,20	4,316	-34,72
1	TiCu	37,15	46,71	-25,72	0,15	0,17	-11,80	3,57	6,52	-82,86
2	TiCu	62,93	39,23	37,67	0,15	0,08	47,68	11,84	11,291	4,66
3	TiCu	47,95	27,22	43,22	0,08	0,07	5,55	10,15	9,467	6,73
4	TiCu	51,13	46,48	9,10	0,17	0,23	-41,27	3,41	0,312	90,85
5	TiCu	64,68	55,88	13,59	0,50	0,23	54,40	2,99	5,619	-88,09

The results obtained from the validation experiments reveal that the results obtained from the generated mathematical models mostly fit the experimental results. Similar outcomes were also obtained from the rest of the diameters. Thus, these empirical equations can easily be used to calculate MRR, EWR and Ra for given EDM drilling process parameters. Nevertheless, there are some results with high percentage errors and these errors might be due to the fact that the empirical models do not fit. The reasons of this lack of fit problem could either come from unstable experimental conditions, improper drilling applications and improper measurements or incorrect mathematical models.

CHAPTER 5

DISCUSSIONS and CONCLUSIONS

This work aims to investigate the EDM hole drilling process which is practically used for aerospace applications and increase the efficiency of this process via optimisation attempts. To do that, an extensive experimental work was developed and conducted. The diameters to be drilled in the experiments were determined in micro and macro levels (0.4 – 3mm). The literature has been reviewed and the frame of the work was shaped. In order to conduct the experiments correctly and accurately, an experimental set-up was prepared, the experiments were designed via statistical techniques and accurate measurement tools/software and equipments were used.

Modelling of the EDM drilling process and the optimisation attempts were the main tasks in the work. To do so, statistical techniques were used to generate mathematical models, reveal the relations of EDM process parameters with outputs and optimisations. The optimisation attempts were implemented to all of the diameters and the results were verified with the validation experiments. The results obtained from the validation experiments revealed that the generated mathematical models can be used to calculate EDM drilling outputs with some exceptions. Some of the models should be regenerated and verified with additional experimental works.

The main effects and the interaction plots indicate the relations between EDM drilling process parameters and the outputs (Appendix C). These plots were analysed and the following conclusions were drawn for EDM micro and macro hole drilling operations;

- I, Ton and C were the main parameters that affected the MRR particularly for all the diameters. However, MRR was adversely affected by increasing these factors on Ti-6Al-4V alloy while drilling of 0.8, 0.7, 0.6, 0.5 and 0.4 diameters. Toff was the only factor that increasing of its setting decreased or had no effect on MRR for all diameters, materials and electrodes.

- EWR increased with increasing discharge current. Ton seemed that it had minor effects on EWR for macro diameters (>1mm) and major effects for micro diameters (< 1mm). Capacitance had substantial role on increasing EWR for the diameters 0.9-3mm. However, increase in C decreased EWR for the diameters 0.8-0.4mm particularly using with copper electrodes on Ti-6Al-4V. Toff seemed an idle factor for the diameters 2, 2.5, and 3mm. For the rest of the diameters, increase in Toff decreased EWR.
- Surface roughness was the primary concern when implementing optimisation and mathematical modelling procedures. Unlike the comments made on MRR and EWR results, the effects of the input factors on Ra were almost opposite. For instance, increasing of discharge current and capacitance produced smooth surfaces without an exception of diameters, materials and electrodes. Ton was not effective on Ra for macro holes, but it showed fairly increasing effect for micro diameters. Similarly, Toff had almost no effect on surface quality of the drilled macro holes. It was limited increasing effect on the diameters 0.6, 0.5 and 0.4 mm.

Other main conclusions drawn from the experimental investigations of EDM fast hole drilling of aerospace alloys are as follows:

- An extensive experimental work was performed using EDM fast hole drilling process on aerospace alloys, namely Inconel 718 and Ti-6Al-4V.
- The experimental investigation covered eleven diameters (0.4, 0.5, 0.6, 0.7, 0.8, 0.9, 1, 1.5, 2, 2.5, and 3mm) which are commonly used in the industrial applications. The diameters between 0.4, 0.5, 0.6, 0.7 and 0.8mm are also accepted as micro hole diameters.
- Mathematical models were generated in order to calculate EDM hole drilling responses using any process parameters. These mathematical can be used to predict the responses for an EDM drilling operation on aerospace alloys.
- Optimum EDM hole drilling settings, MRR, EWR, surfaces roughness, and drilling time were all determined and verified for the eleven diameters, two alloys and electrode materials.

REFERENCES

[1] Qu and J. (2002), Development of cylindrical wire electrical discharge machining process and investigation of surface integrity and mechanical property of EDM surface layers, *PHd Thesis, North Carolina State University*

[2] Puranik M.S. and Joshi S.S.(2005), Analysis of accuracy of high-aspect-ratio holes generated using micro-electric discharge machining drilling, *Proc. IMechE Vol. 222 Part B: J. Engineering Manufacture*

[3] Kalpakjian S. (2010), *Manufacturing engineering and technology*, Prentice Hall, 6th Edition, Singapore, , Pp. 769

[4] Ergün and Çoğun (2006), Elektro erozyon ile işleme (EEİ) iş parçası yüzey karakteristiklerinin deneysel incelenmesi, *Gazi Üniv. Müh. Mim. Fak. Der.,* **21,3**, 427-441

[5] Khan A.A. (2008), Electrode wear and material removal rate during EDM of aluminum and mild steel using copper and brass electrodes, *Int. J. of Adv Manuf. Technol.,* **39**, 483-487

[6] Hasçalık and Çaydaş (2007), Electrical discharge machining of titanium alloy (Ti-6Al-4V), *Applied Surface Science* **253**, 9007-9016.

[7] Tomadi S.H (2009), Analysis of the influence of EDM parameters on surface quality, material removal rate and electrode wear of tungsten carbide, , *IMECS 2009, 2, March 18-20, Hong Kong,*

[8] Habib S.S. (2009), Study of the parameters in electrical discharge machining through response surface methodology approach, *Applied mathematical modeling* **33**, 4397-4407

[9] Deniz and Çoğun (2005), Elektro erozyonla işlemede işleme parametrelerinin matematiksel modellenmesi, *Makine Tasarım ve İmalat Dergisi* Cilt **7**, Sayı 1, Mayıs

[10] Tsai M. and Wang J. (2001), Semi-empirical model of surface finish on electrical discharge machining, *International Journal of Machine Tools & Manufacture* **41** 1455-1447

[11] Pradhan B.B. (2009), Investigation of electro-discharge micro-machining of titanium super alloy, *Int J Adv Manuf Technol Int. J. Adv. Manuf. Tech.,* **41**, 1094-1106

[12] Yan B.H. and Huang F.Y. (1999), Micro-hole machining of carbide by electric discharge machining, *Journal of Materials Processing Technology* **87139**-145

[13] Leao F. and Pashby I. (2005), Optimization of EDM fast hole drilling through an evaluation of electrode geometry. *18th International Congress of Mechanical Engineering* November 6-11, Ouro Preto, MG

[14] Bigot S., Micro EDM parameters optimization.

[15] Soni J.S. (1993), Surface characteristic of titanium with rotary EDM, *Bull. Mater. Sci.,***16-** 3, pp. 213-227,

[16] Kuppan P. (2008), Influence of EDM process parameters in deep hole drilling of Inconel 718, *Int. J. Adv. Manuf. Tech.,* **38**, 74-84,

[17] Wang C.C. and Yan B.H. (2000), Blind-hole drilling of Al_2O_3/6061Al composite using rotary electro-discharge *machining, Journal of Materials Processing Technology* **102**, 90-102

[18] Leao F. and Pashby I. (2005), Optimization of EDM fast hole drilling through an evaluation of dielectric and electrode materials, *18th International Congress of Mechanical Engineering* November 6-11, Ouro Preto, MG

[19] Kumagai S. and Sato N. (2007), Operation parameter optimization for fabrication of a narrow deep hole in metal by electrical discharge machining using a dielectric-encased wire electrode, *Journal of Materials Processing Technology* **189**, 310-315

[20] Jahan M.P. and Wong Y.S. (2009), A study on the quality micro-hole machining of tungsten carbide by micro-EDM process using transistor and RC-type pulse generator, Journal of Materials Processing Technology, **209**, 1706-1716

[21] Montgomery D. C (2001). *,Design and analysis of experiments hand book,* 5^{th} edition, Willey & Sons inc

[22] Fallon M. and Walton A.J. (1995), A comparison of Taguchi methods and response surface methodology for optimizing a cmos process, IEE, Savoy Place, London WC2R 0BL, UK

[23] MINITAB User's Manual, Release 14.0. Documentation for MINITAB

APPENDICES

Appendix A: Main Effect Graphs for D2 hole

Appendix B: Interaction Graphs for D2 hole

Appendix C: General rules of EDM hole drilling process parameters on the responses

Appendix A

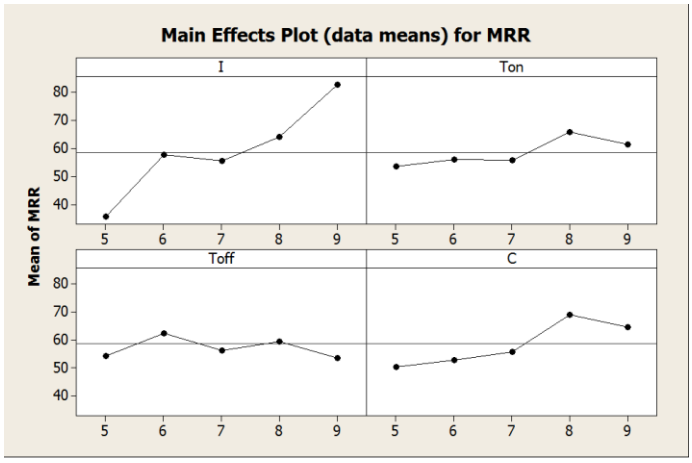

Figure A.1 D2NiCu MRR Main Effects Graphs

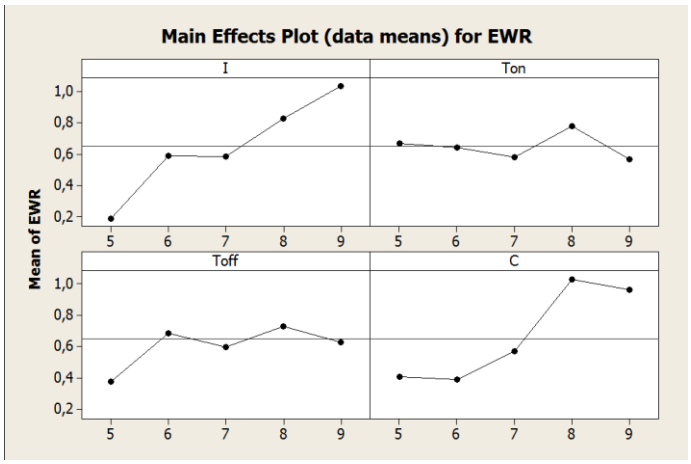

Figure A.2 D2NiCu EWR Main Effects Graphs

Figure A.3 D2NiCu Ra Main Effects Graphs

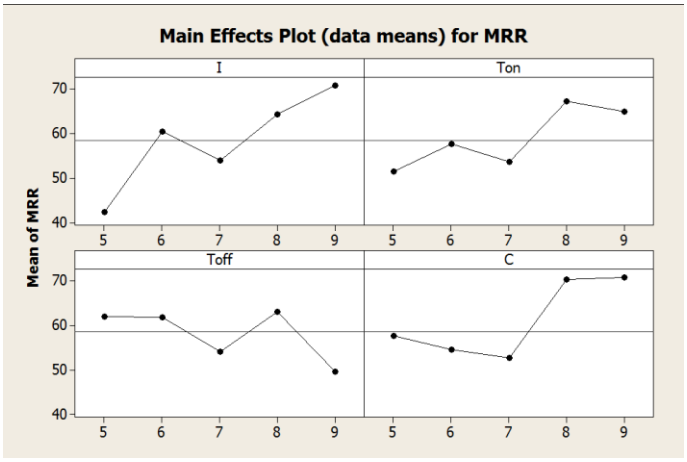

Figure A.4 D2TiBr MRR Main Effects Graphs

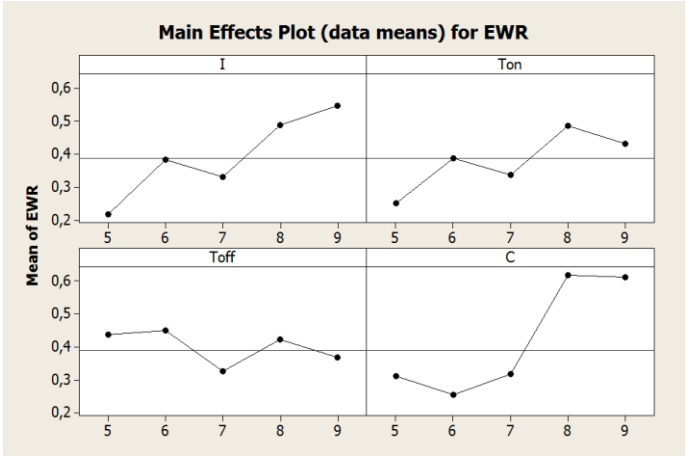

Figure A.5 D2TiBr EWR Main Effects Graphs

Figure A.6 D2TiBr Ra Main Effects Graphs

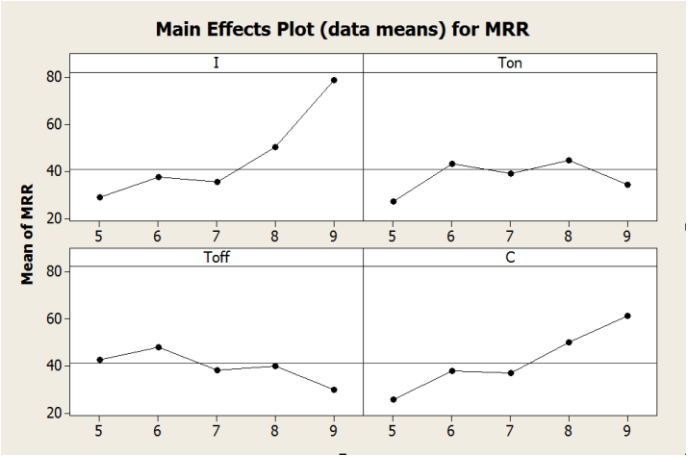

Figure A.7 D2TiCu MRR Main Effects Graphs

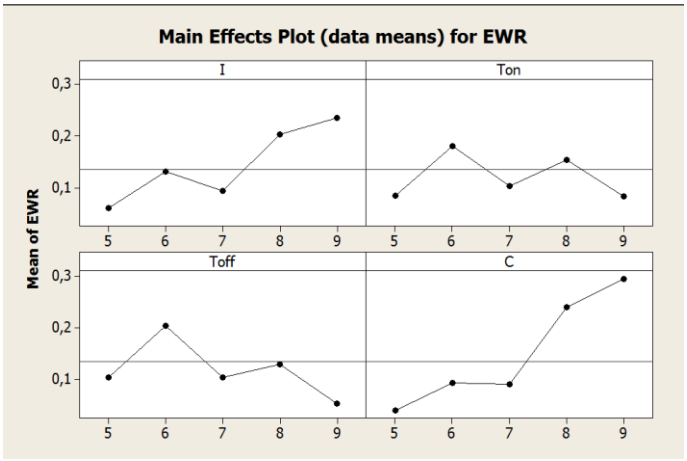

Figure A.8 D2TiCu EWR Main Effects Graphs

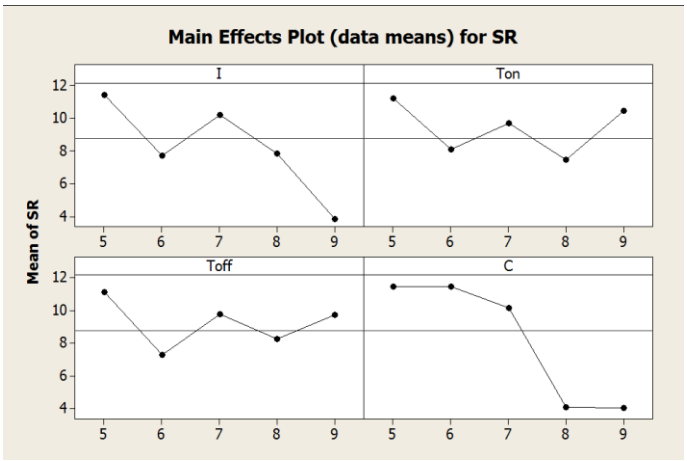

Figure A.9 D2TiCu Ra Main Effects Graphs

Appendix B

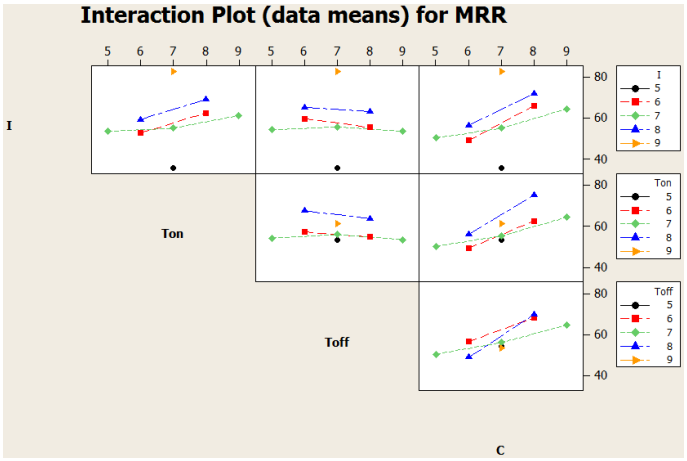

Figure B.1 Interaction Graphs of D2NiCu MRR

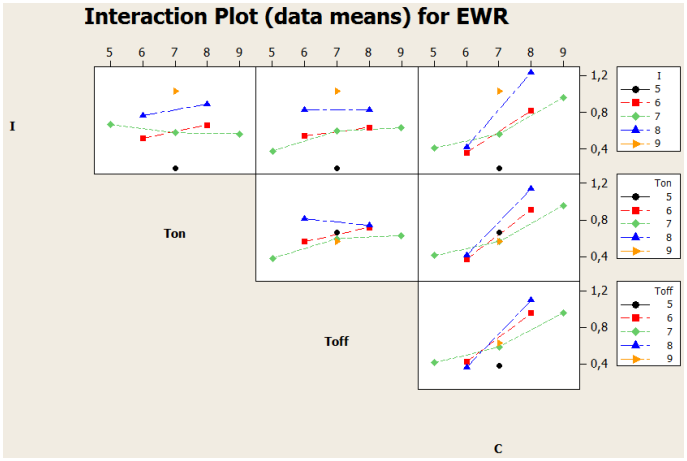

Figure B.2 Interaction Graphs of D2NiCu EWR

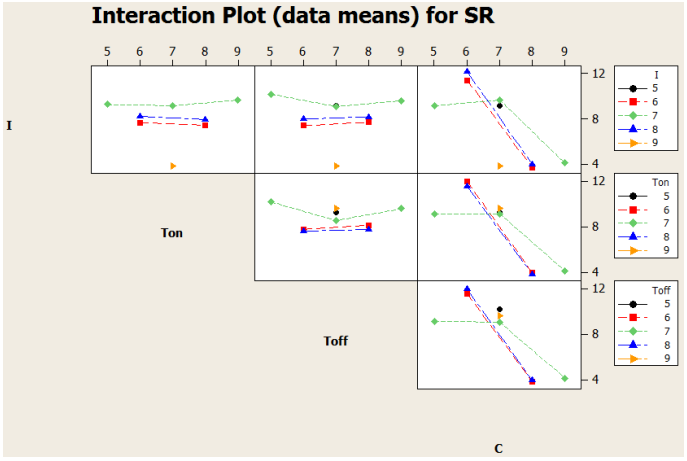

Figure B.3 Interaction Graphs of D2NiCu Ra

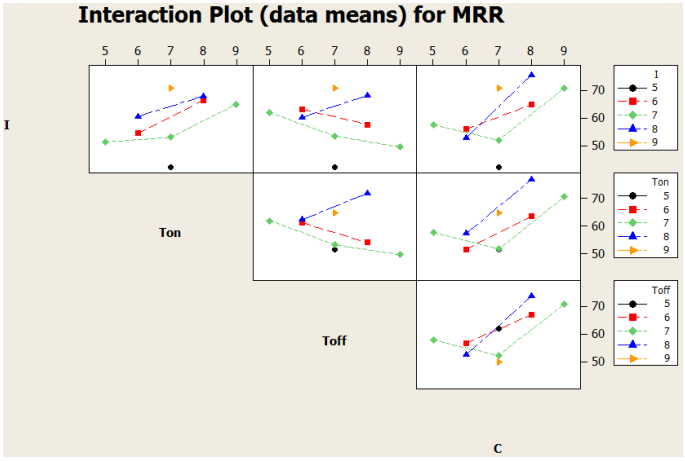

Figure B.4 Interaction Graphs of D2TiBr MRR

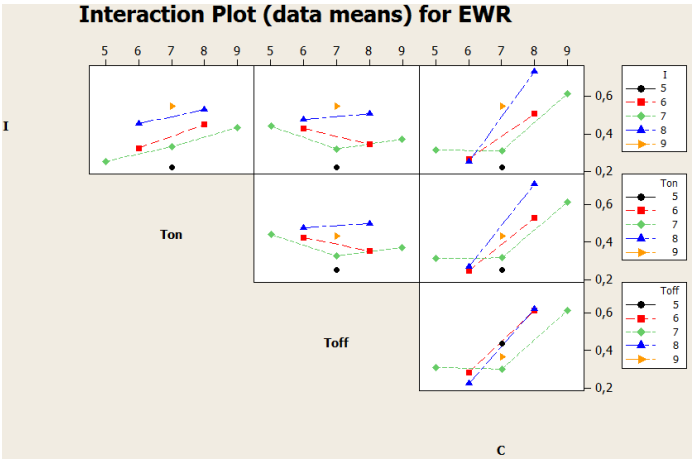

Figure B.5 Interaction Graphs of D2TiBr EWR

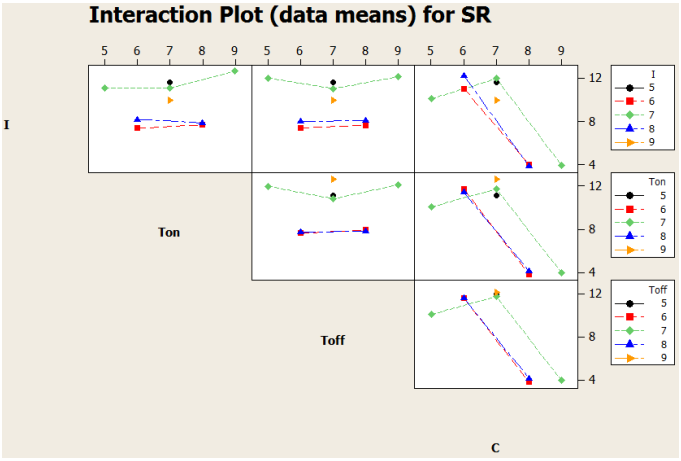

Figure B.6 Interaction Graphs of D2TiBr Ra

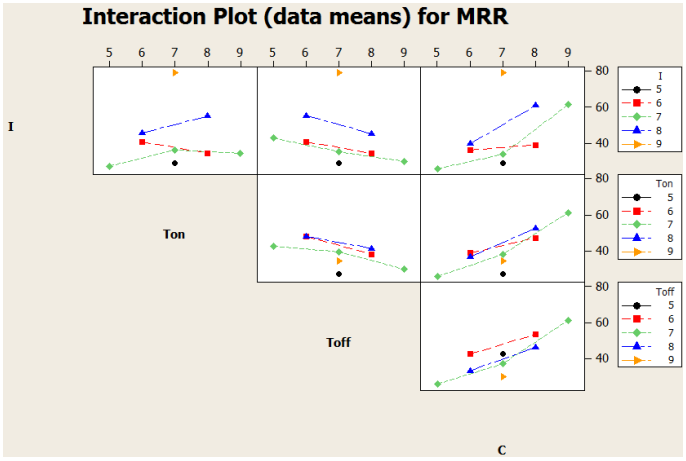

Figure B.7 Interaction Graphs of D2TiCu MRR

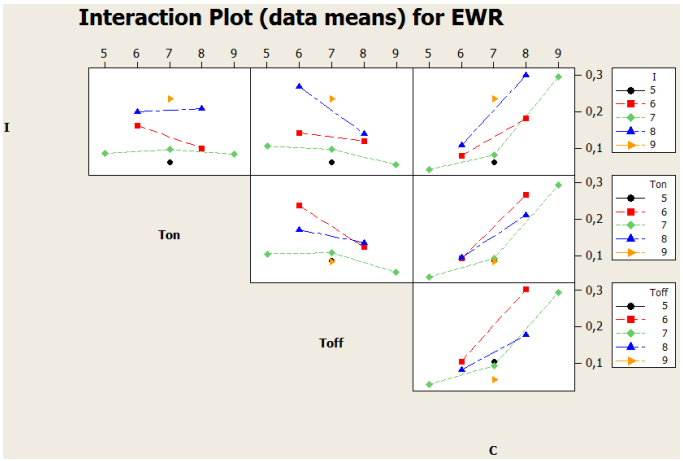

Figure B.8 Interaction Graphs of D2TiCu EWR

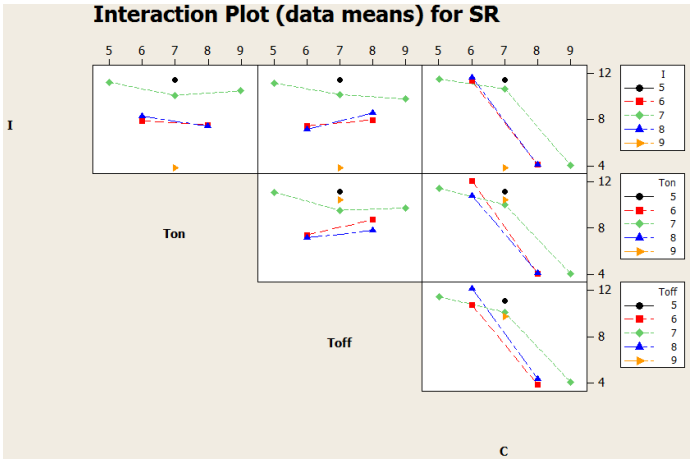

Figure B.9 Interaction Graphs of D2TiCu Ra

Appendix C

Table C.1 General rules of EDM hole drilling process parameters on the responses

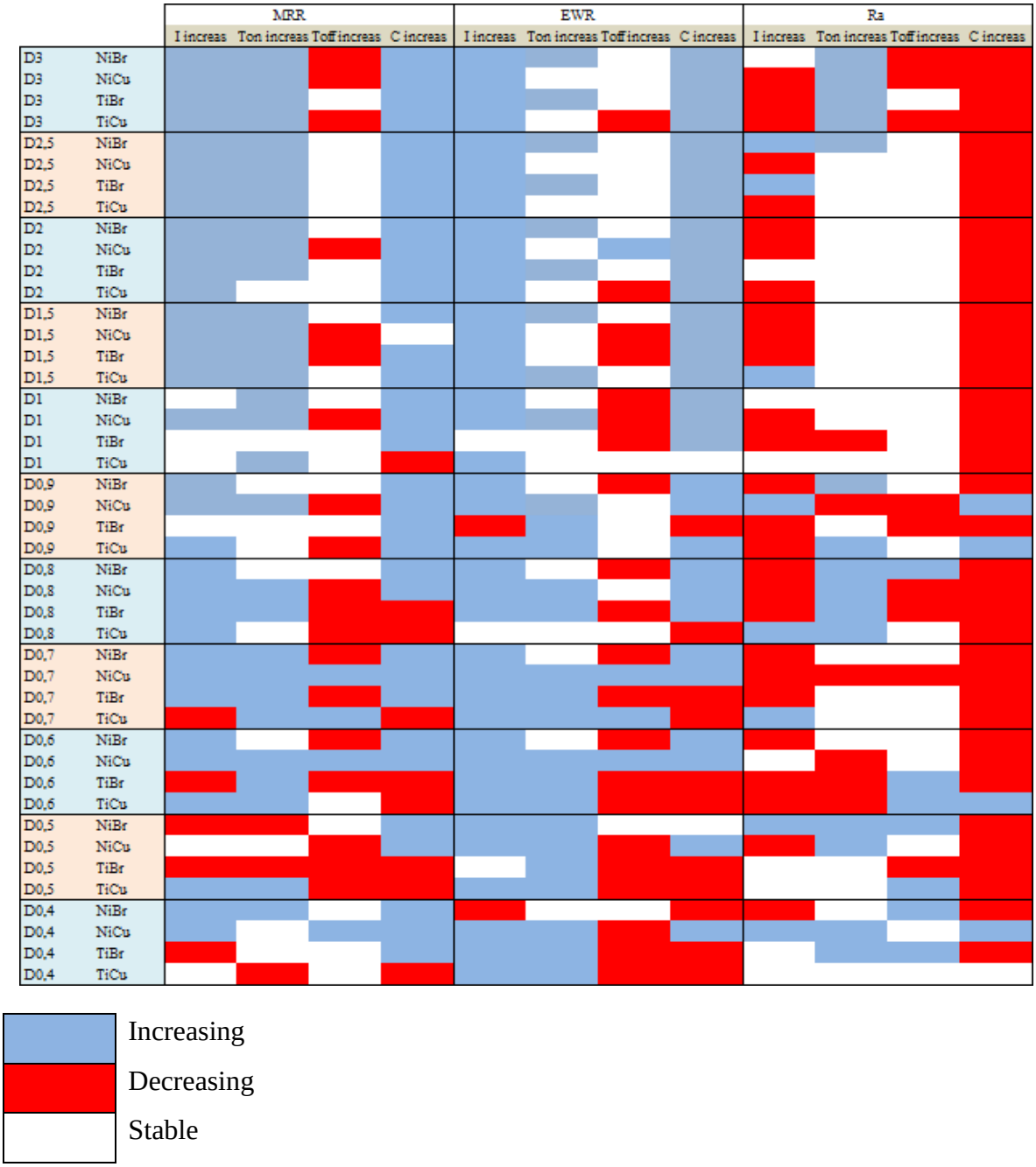

LIST OF PUBLICATIONS

International SCI-Expanded Journal Papers:

1. Oguzhan Yilmaz and M.Ali Okka, Effect of single and multi-channel electrodes application on EDM fast hole drilling performance, International Journal of Advanced Manufacturing Technology, v 51, n 1-4, p 185-195, 2010

International Refereed Conference Papers:

1. Oguzhan Yilmaz, A. Tolga Bozdana, M.Ali Okka, I. Huseyin Filiz, An intelligent and automated system for EDM drilling of super alloys, Proceedings' of 5th International Conference on Responsive Manufacturing, Green Manufacturing, ICRM 11-13 January 2010, The University of Nottingham Ningbo, China, ISBN: 978-1-84919-199-9, pp.95-99

2. A.Tolga Bozdana, Oguzhan Yilmaz, M.Ali Okka, I.Huseyin Filiz, Mathematical modelling of EDM hole drilling using response surface methodology, Proceedings of 5th International Conference on Responsive Manufacturing, Green Manufacturing, ICRM 11-13 January 2010, The University of Nottingham Ningbo, China, ISBN: 978-1-84919-199-9, pp.90-94

3. O.Yilmaz, A.T. Bozdana, M.A. Okka, İ.H. Filiz, A comparative investigation of the effects of single and multi-channel electrodes in EDM fast hole drilling of aerospace alloys, 5th International Conference and Exhibition on Design and Production of Machines and Dies/Molds, 18-21 June 2009, Kuşadası, Aydın, Turkey. pp. 223-227, ISBN: 978-605-60732-0-5.

4. A.T. Bozdana, O.Yilmaz, M.A. Okka, İ.H. Filiz, A comparative experimental study on fast hole EDM of Inconel 718 and Ti-6Al-4V, 5th International Conference and Exhibition on Design and Production of Machines and Dies/Molds, 18-21 June 2009, Kuşadası, Aydın, Turkey, pp. 229-232, ISBN: 978-605-60732-0-5.

National Refereed Journal Paper:

1. Oğuzhan Yılmaz, A.Tolga Bozdana, M.Ali Okka, İ.Hüseyin Filiz, Uzay ve Havacılık Malzemelerinde Elektriksel Erozyon ile Hızlı Delik Delme Performansının Deneysel İncelenmesi, Mühendis ve Makina, Eylül 2010, Sayı:608, ISSN: 1300-3402.

National Congress Paper:

1. Oğuzhan Yılmaz, A.Tolga Bozdana, M.Ali Okka ve İ.Hüseyin Filiz, Uzay ve havacılık malzemelerinde elektriksel erozyon ile hızlı delik delme performansının incelenmesi, TMMOB Makina Mühendisleri odası Konya Şubesi, V. Makina Tasarım ve İmalat Teknolojileri Kongresi, 17-18 Ekim 2009, Bildiri Kitabı, sayfa: 211-218, Konya, ISBN: 978-9944-89-771-6, MMO Yayın no: E/209/510-1.

2. Oğuzhan Yılmaz, A.Tolga Bozdana, M.Ali Okka, Uzay ve havacılık uygulamalarında kullanılan nikel ve titanium alaşımlı malzemelerde elektriksel erozyon işlemi kullanılarak hızlı delik delme, Makine İmalatı Sektöründe Ar-Ge Proje Pazarı-Gaziantep Sanayi Odası, 25-26 Mart 2010. Bildiri Kitapçığı.